

2359-12

**Joint ICTP-IAEA Workshop on Physics of Radiation Effect and its Simulation
for Non-Metallic Condensed Matter**

13 - 24 August 2012

JRC testing facilities and experimental tools for study of radiation damage

Thierry Wiss
*Joint Research Centre, European Commission
Eggenstein
Germany*

JRC testing facilities and experimental tools for study of radiation damage

Thierry Wiss

The European Commission's in-house science service

www.jrc.ec.europa.eu



*Serving society
Stimulating innovation
Supporting legislation*



JRC testing facilities and experimental tools for study of radiation damage

TMS + MMSNF

Studies on properties and behaviour of nuclear fuels



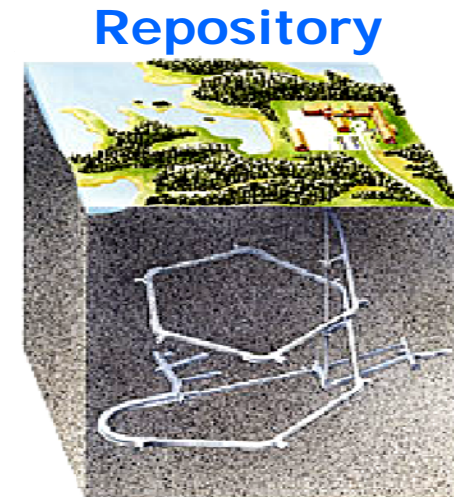
*European Commission, Joint Research Centre,
Institute for Transuranium Elements
P.O. Box 2340, 76125 Karlsruhe, Germany.
thierry.wiss@ec.europa.eu*



Content



- Forewords
- PIE
- Studies on spent fuel
- Cladding
- Conclusion / perspectives



Scope



waste composition/irradiation history

Aging: solid state
radiation damage mechanisms, effects

helium accumulation

property evolution
- bulk
- interface

microstructure evolution
oxidation
recovery (annealing)

High-level wastefoms:

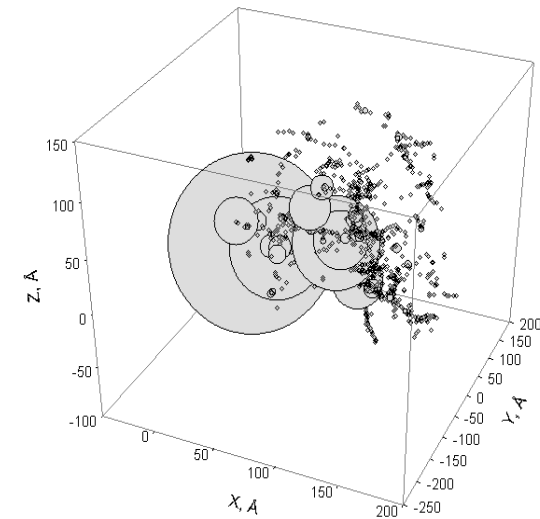
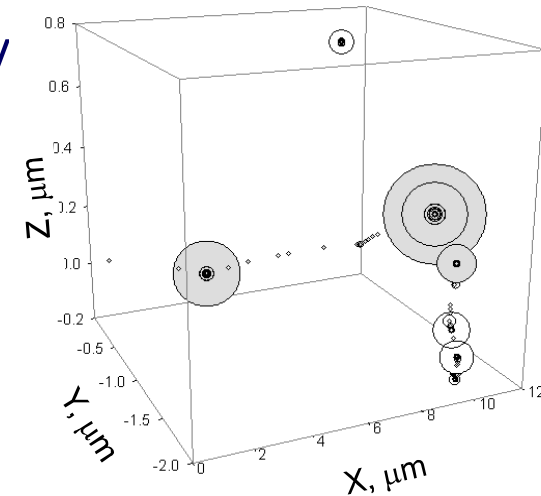
**high bu UO_2
MOX
new compounds
(crystalline) conditioning matrices**

Timeframes:

short-term
interim (<500 y)
geologic periods

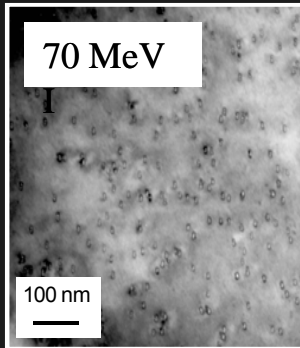
**long term
mechanical stability**

5 MeV alpha-particle

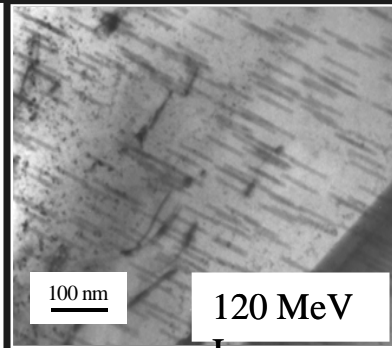


100 keV recoil atom

Methodology

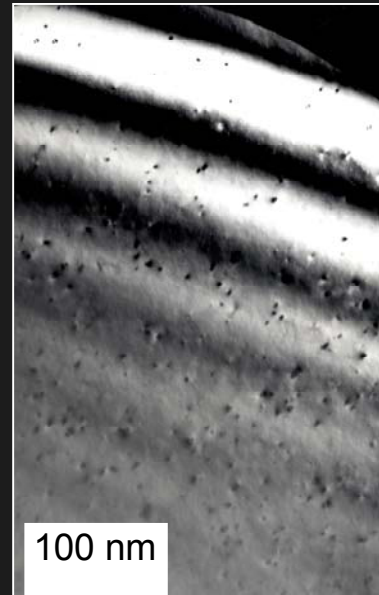


CeO



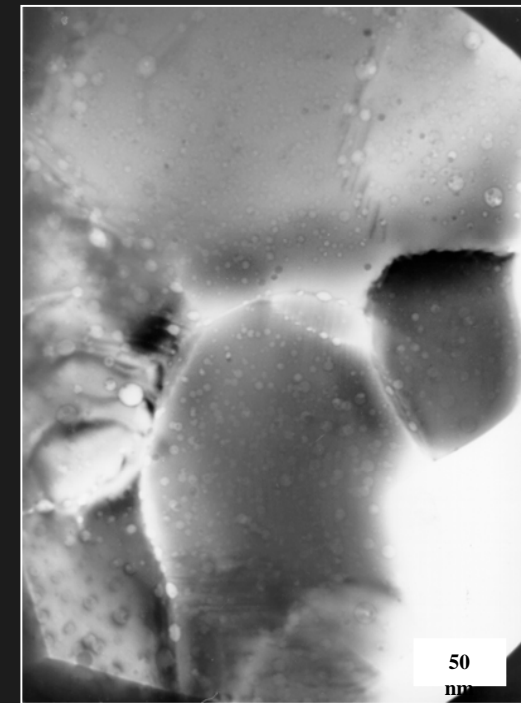
Nd₂Zr₂O

Single effect studies: irradiation with selected ions at given energies



(U, ²³⁸Pu)O₂

Doping with alpha-emitters for homogeneous damage and helium distribution



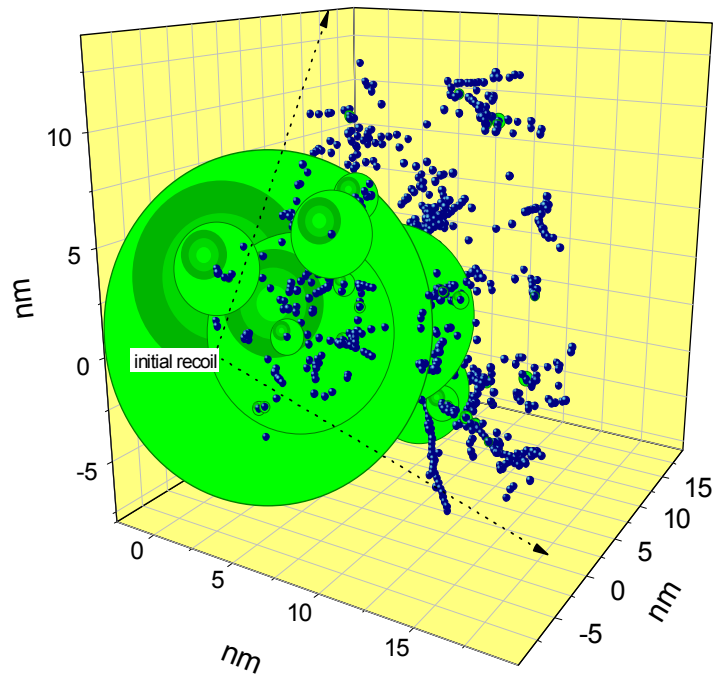
UO₂ - 75 GWd/t_U

Concomittant effect of different damage sources

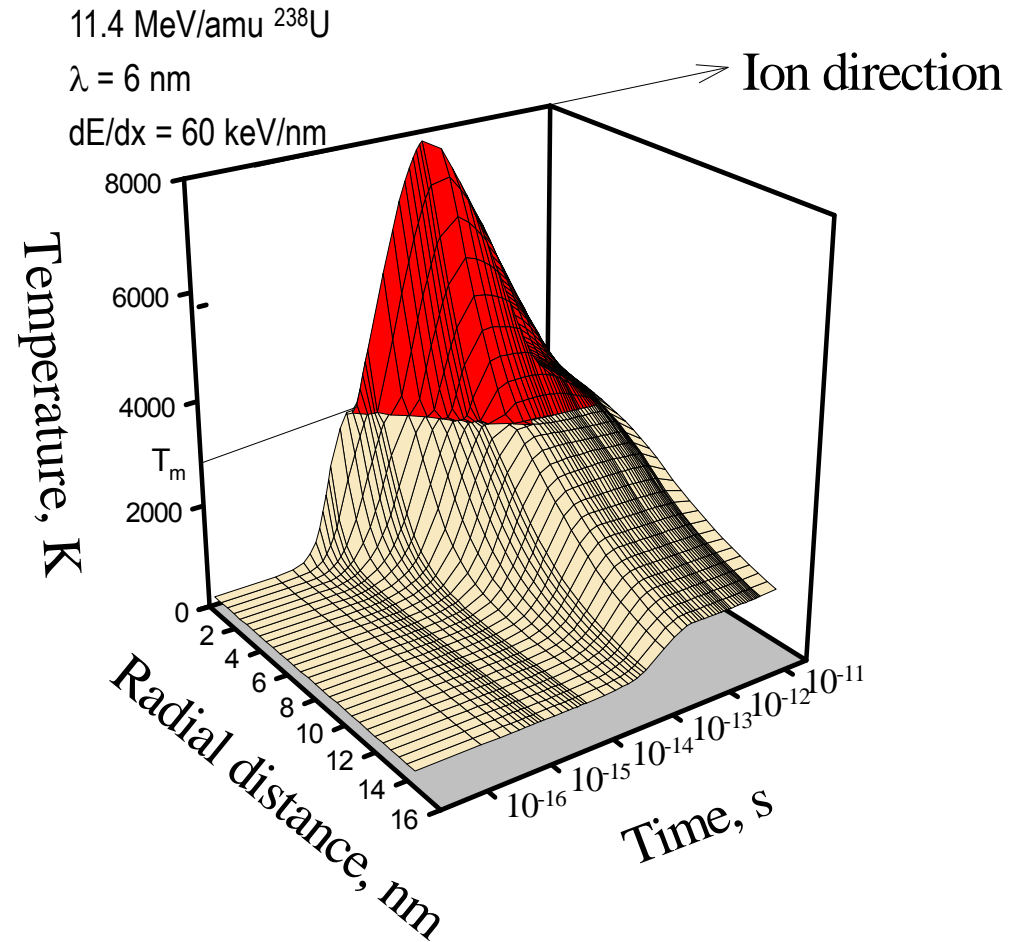
Damage in UO₂



Cascade from a recoil (SRIM2000)



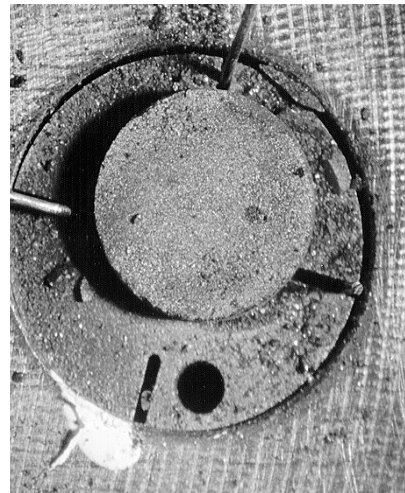
Thermal spike



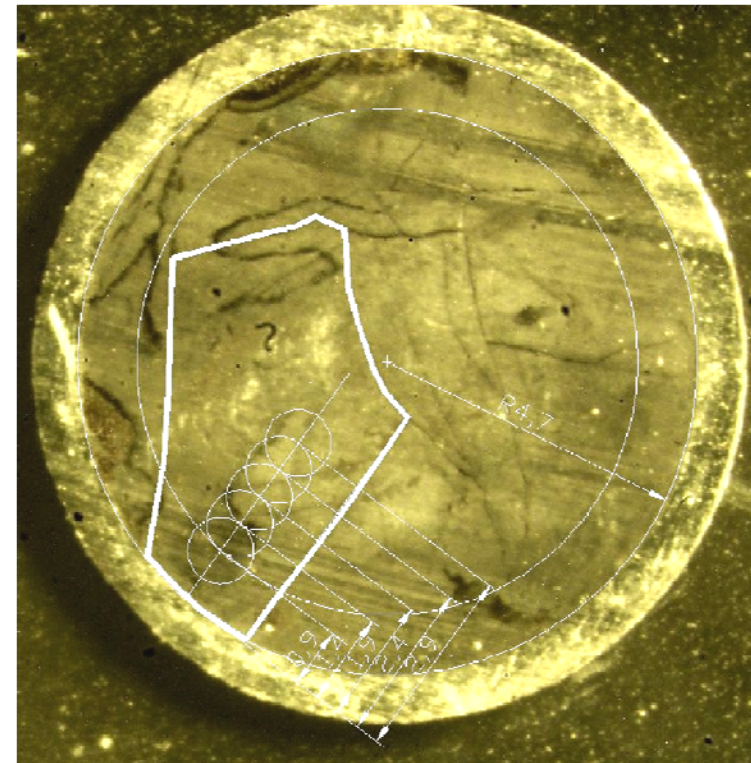


How to measure properties as a function of burnup, T_{irr} ?

The combination of commercial fuel investigations and tailor-made irradiations provides optimum results.



UO₂ discs irradiated to a flat burnup and T_{irr} radial profile.
(HBRP project)



High burnup LWR UO₂ radial averaging of measured quantities; (white circles indicate spots for Laserflash measurements)

Electron microscopy



Tecnai G² F20 XT



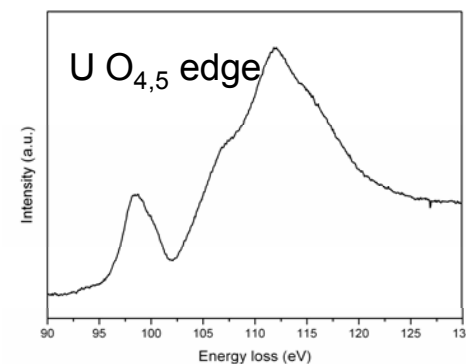
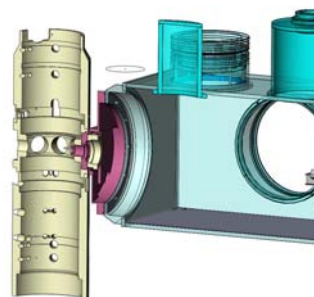
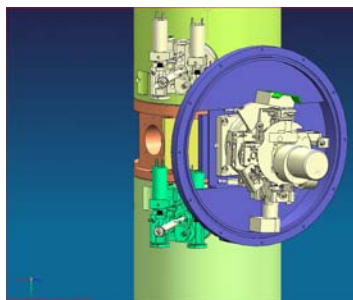
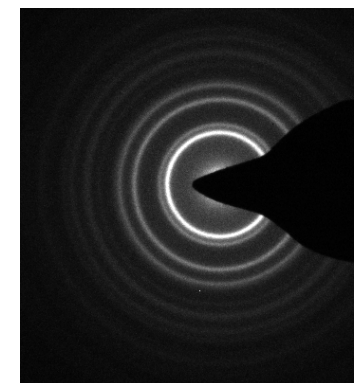
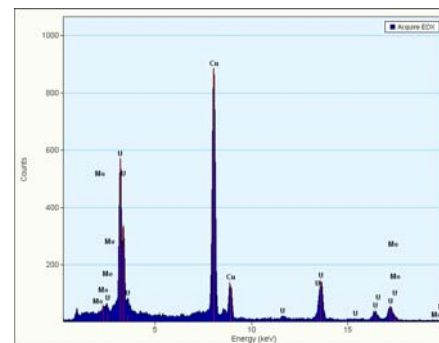
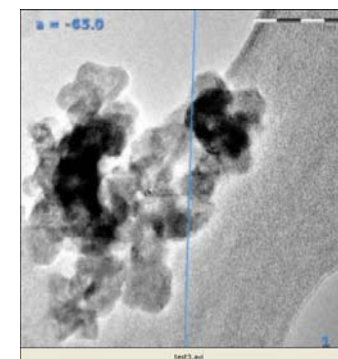
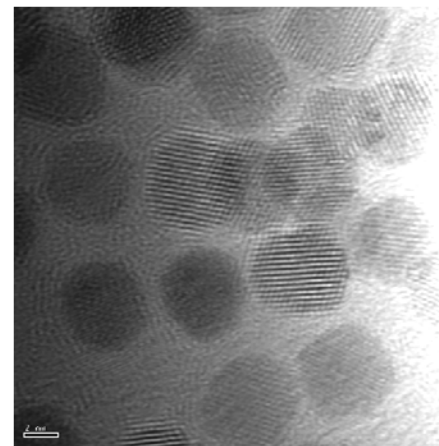
SEM Philips XL40
SE, BSE, EDX

Irradiated fuel can be handled.

TEM characteristics



- TEM point resolution (nm) 0.25
- TEM line resolution (nm) 0.102
- Information limit (nm) 0.14
- TEM magnification range 22 x - 930
- STEM HAADF resolution (nm) 0.23 (0.18)
- STEM magnification range 150 x - 230 Mx
- Maximum tilt angle with tomography holder $\pm 70^\circ$
- EDS energy resolution 134.6 eV
- Spot drift 1 nm.min⁻¹
- Resolution EELS (ZLP) 0.6 eV

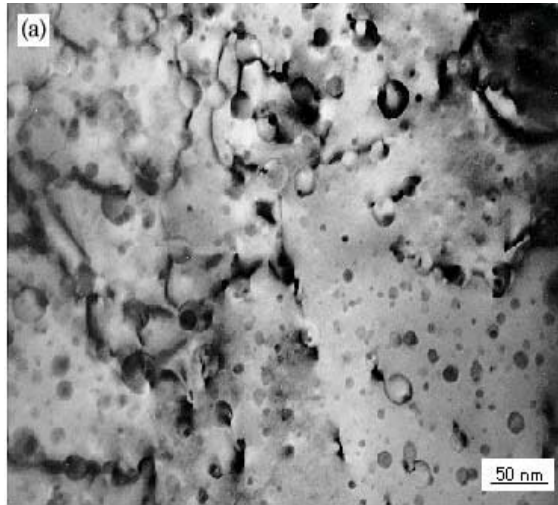


Microstructure of high burnup fuel (TEM)

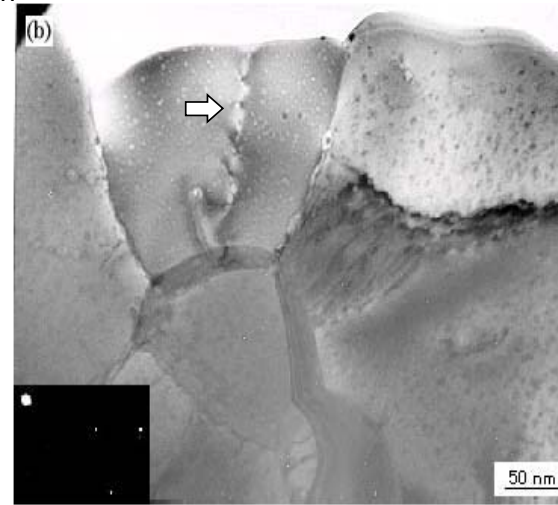


Commission
européenne

LWR $T_{irr} = 450$ C



UO₂ 55 GWd/t



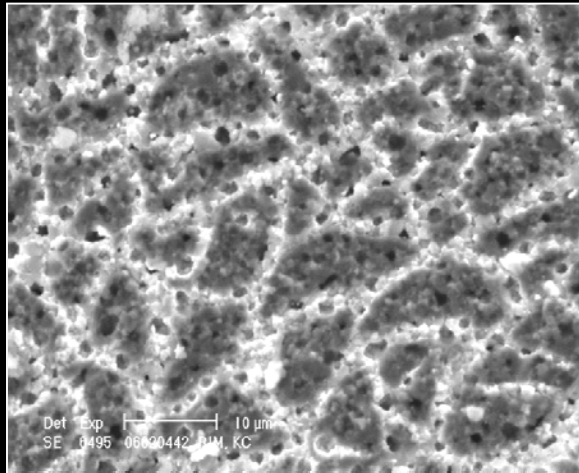
UO₂ 82 GWd/t

Studies on high burnup fuel properties are continuing along several lines:

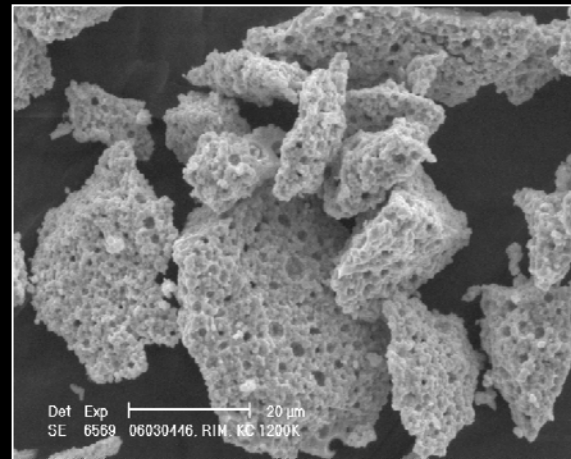
- fundamental studies on (radiation damage) evolution at very high dose/burnup.
- microstructure examination of high burnup fuel to 'map' relevant features and quantify distribution of gas bubbles, extended defects
- effects of accumulated strain energy on the fuel restructuring process

models will be implemented in codes.

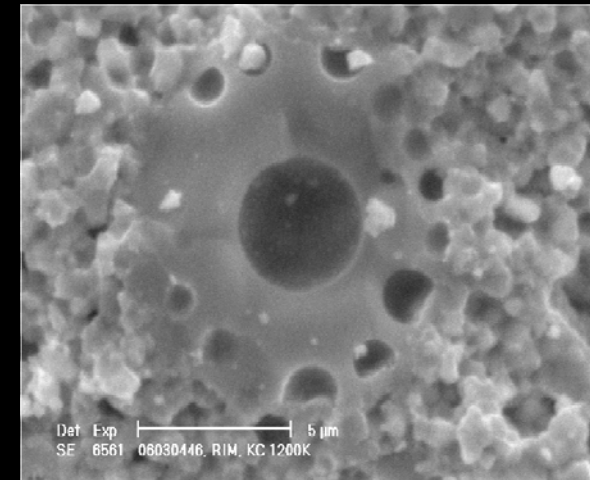
SEM of a 200 GWd/t_U fuel sample



Memory effect after HBS formation



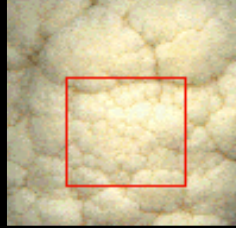
Break of the structure during annealing (1200 K)



Formation of „ultimate“ pores at very high burnup

Fission product release and microstructure changes during laboratory annealing of a very high burn-up fuel specimen, J.-P. Hiernaut *, T. Wiss, J.-Y. Colle, H. Thiele, C.T. Walker, W. Goll, R.J.M. Konings, J.Nucl. Mater., in press

High Burnup Structure



Fractal dimension

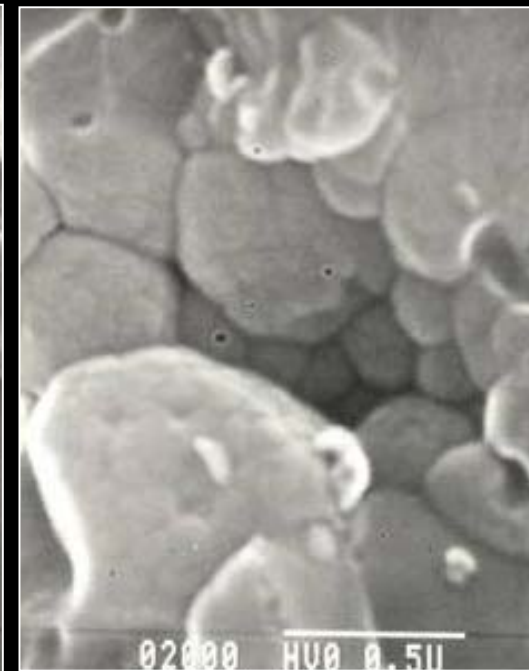
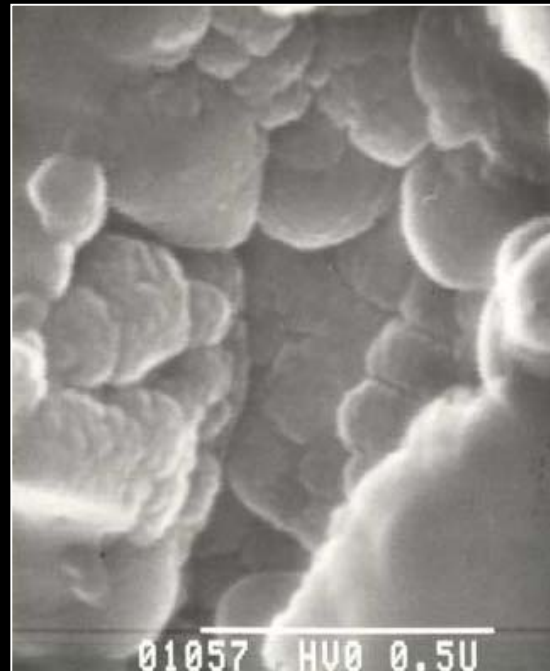
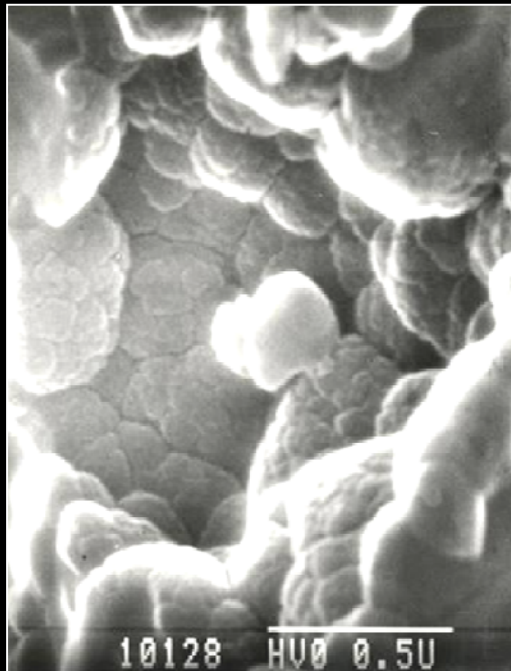
$\log p / \log q$

p: nb of fractals

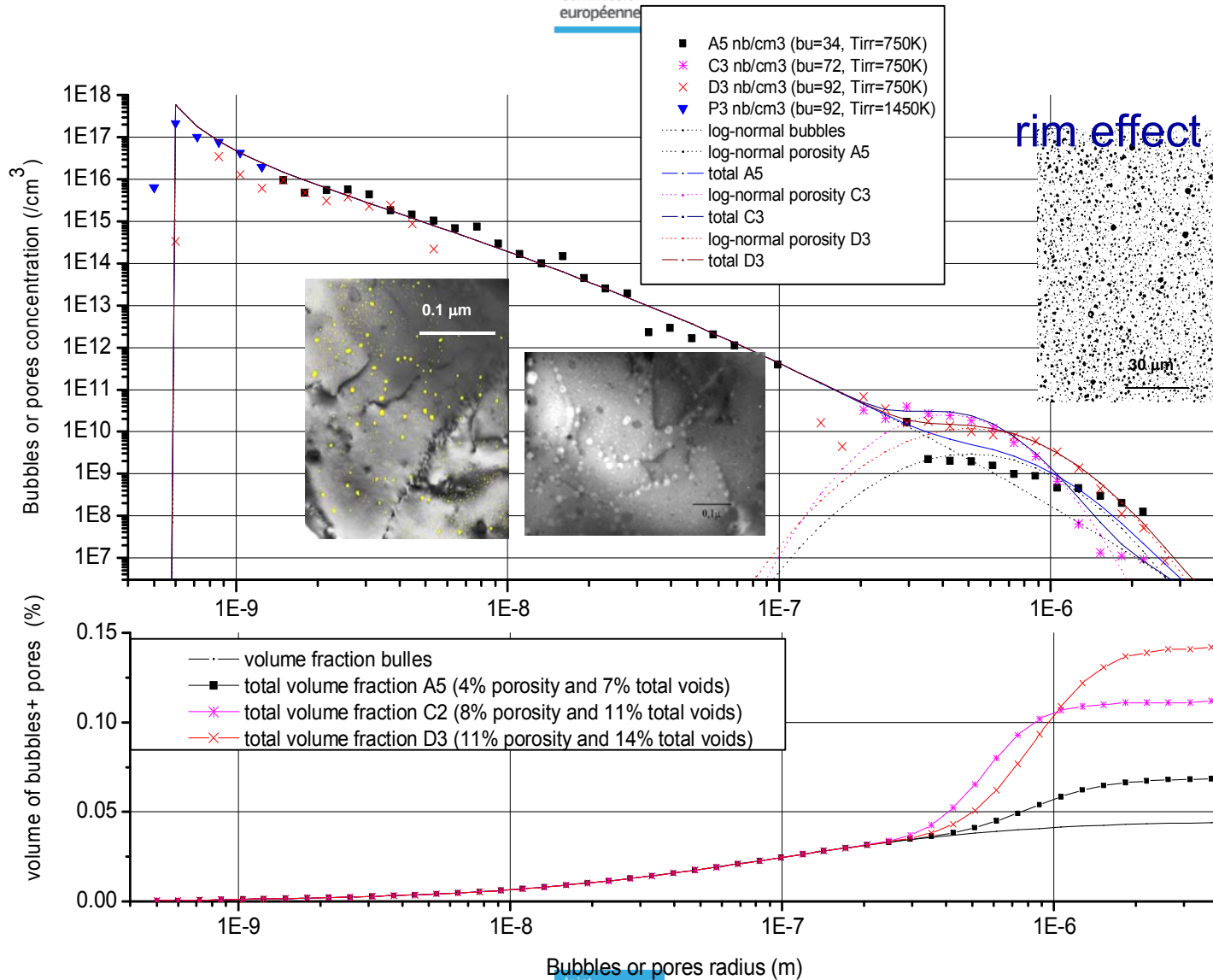
q: magnification

HBS $d = 2.2$

(Cauliflower $d = 2.33$)



fg bubbles and pores in irradiated UO₂



Bubbles or pores radius (m)

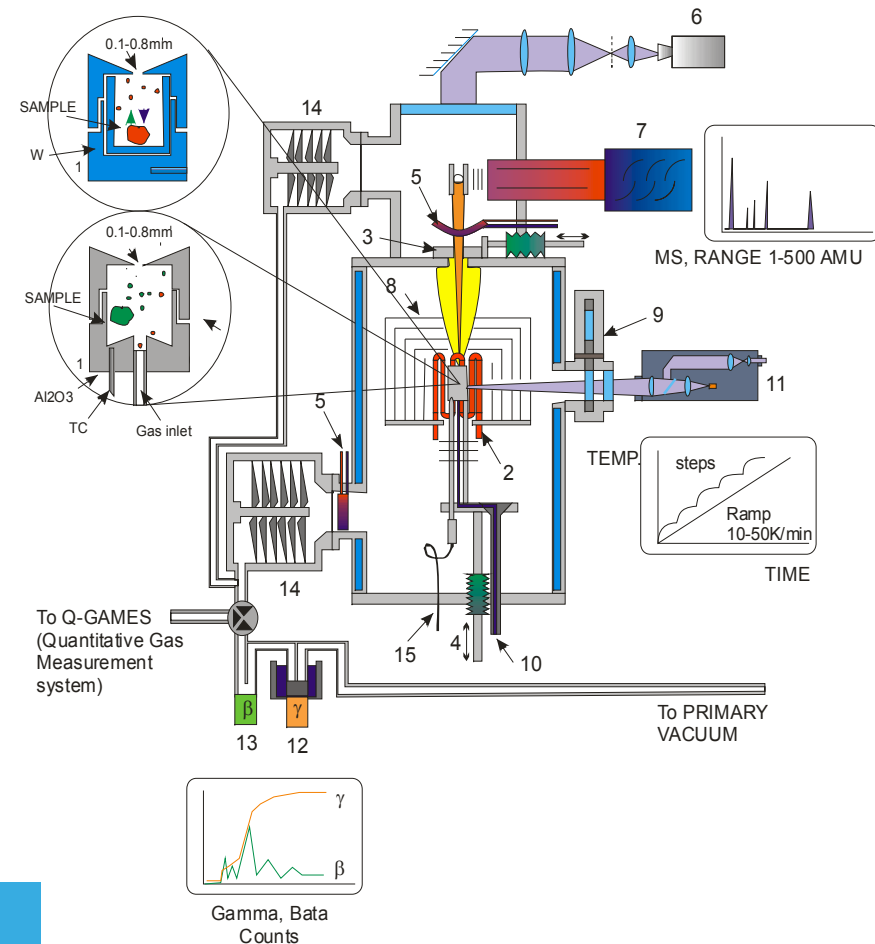
Knudsen cell effusion setup with mass spectrometer

*Various types of cells used
in high vacuum or under controlled, chemically reacting atmosphere up to 3100 K.*

Effusion and release processes from **irradiated fuel** with temperature programs up to complete vaporization of the sample

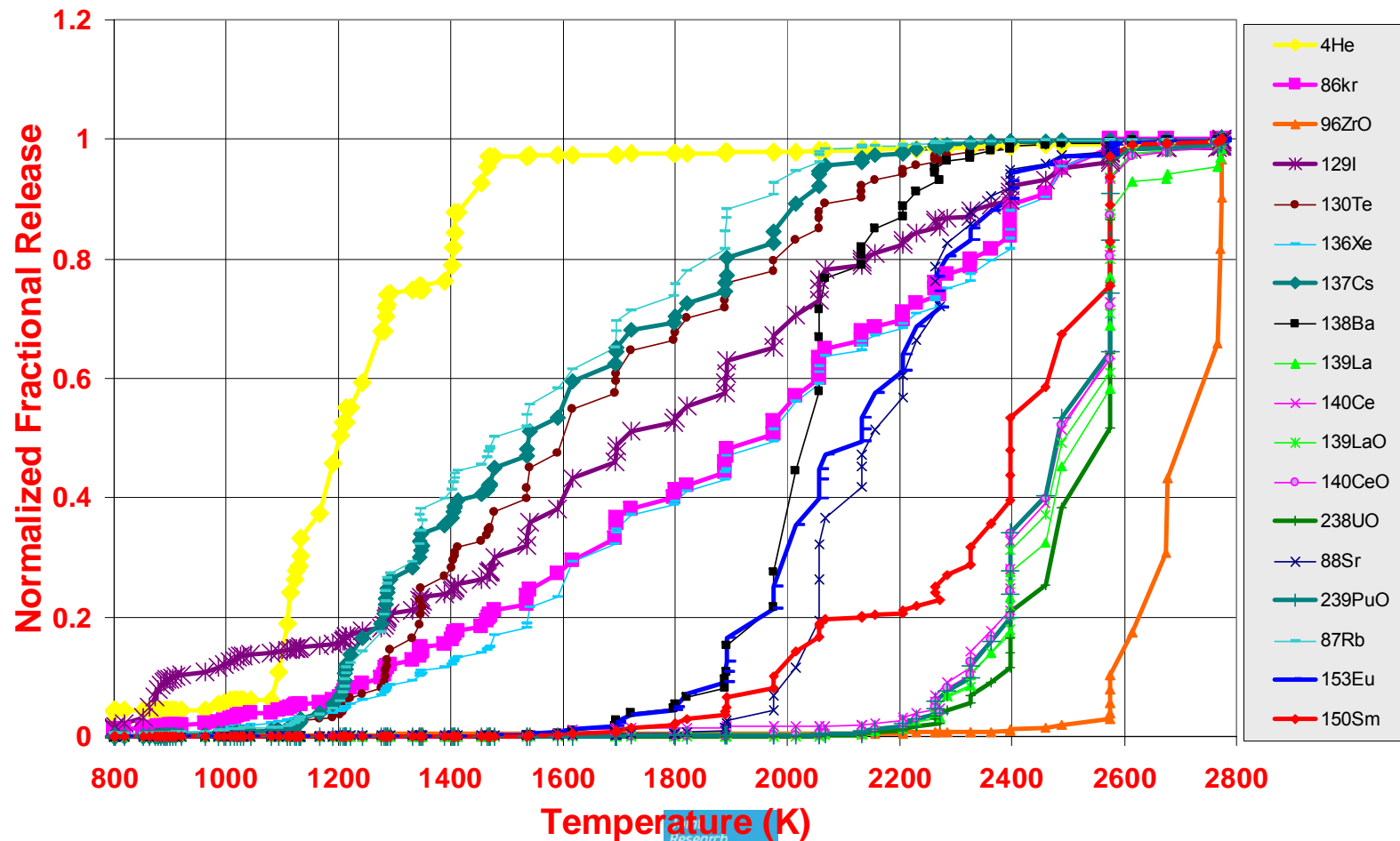
Type of measurements:

- Equilibrium vapour pressure over the fuel
- Composition changes during annealing
- Release behaviour and analysis of He and fg



Fractional release of irradiated UO_2

sample from the central region of the pellet



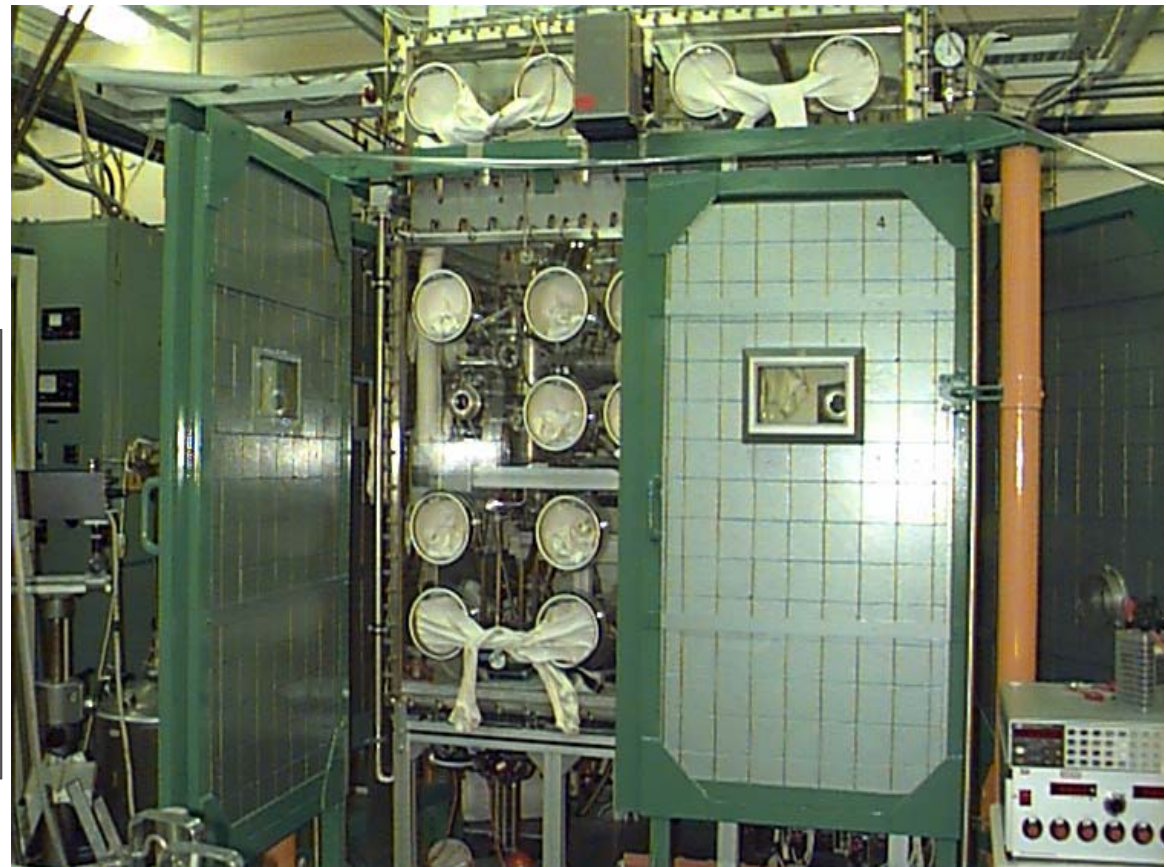
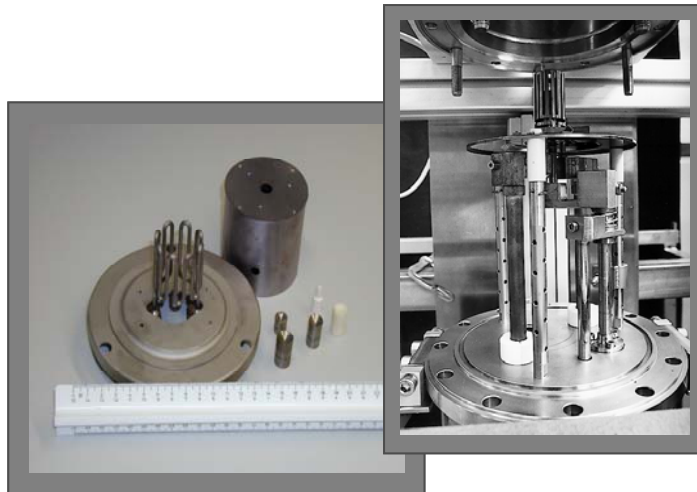
Knudsen cell effusion setup



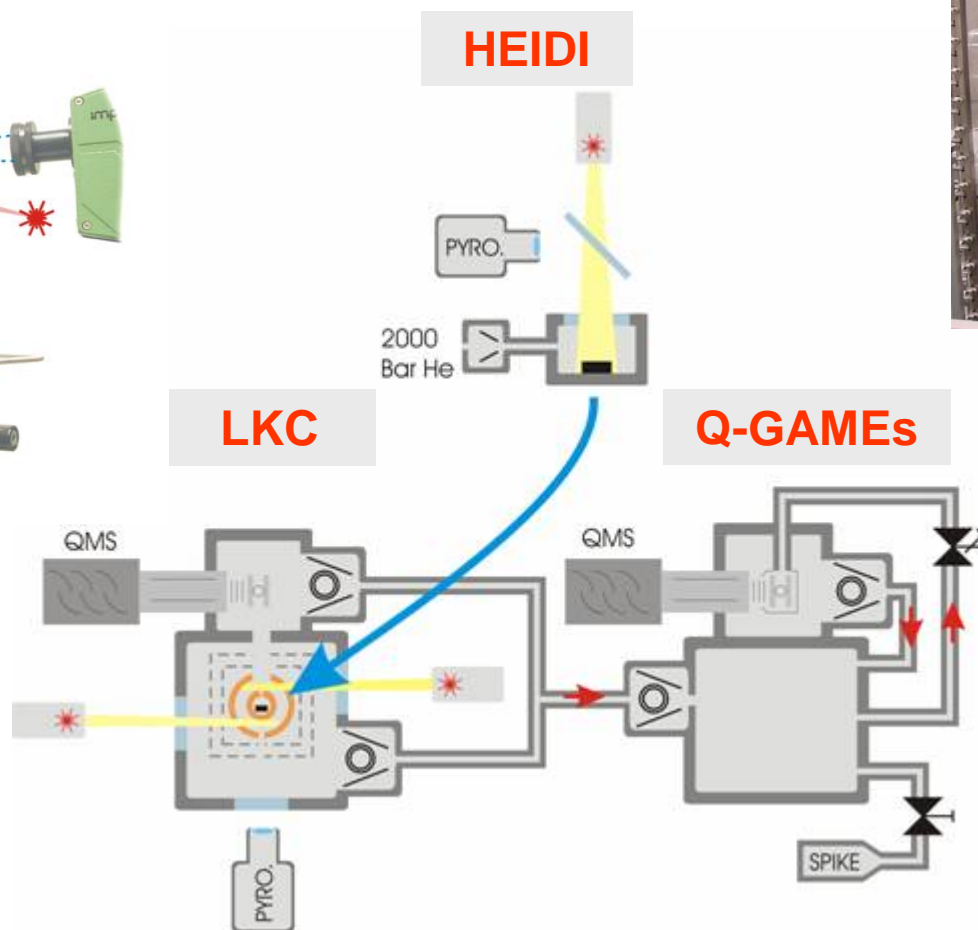
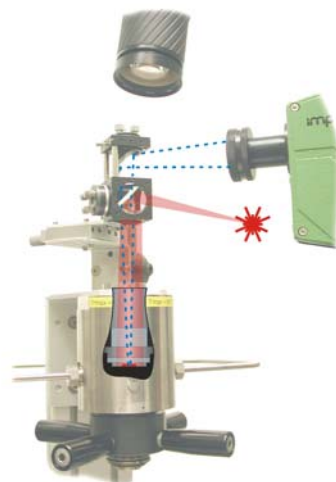
Various types of cells can be used to work in a ultra-high vacuo or in a low-pressure controlled atmosphere up to 3000 K.

The mass-spectrometer noise is less than 10^{-13} A.

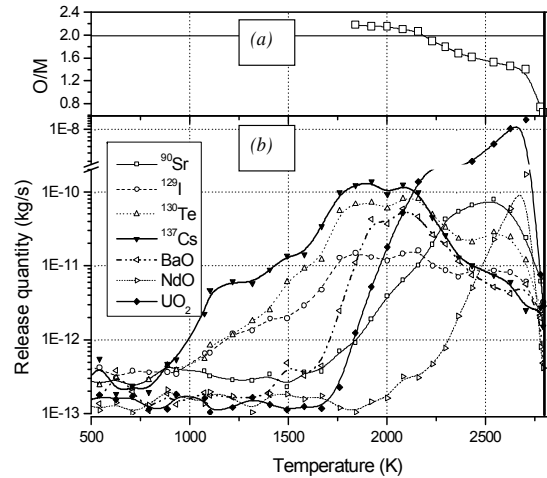
The usable m.s. signal range extends over *six* orders of magnitude.



Q-GAMES

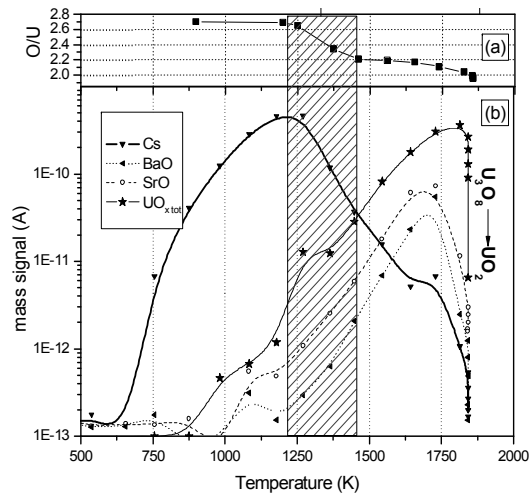
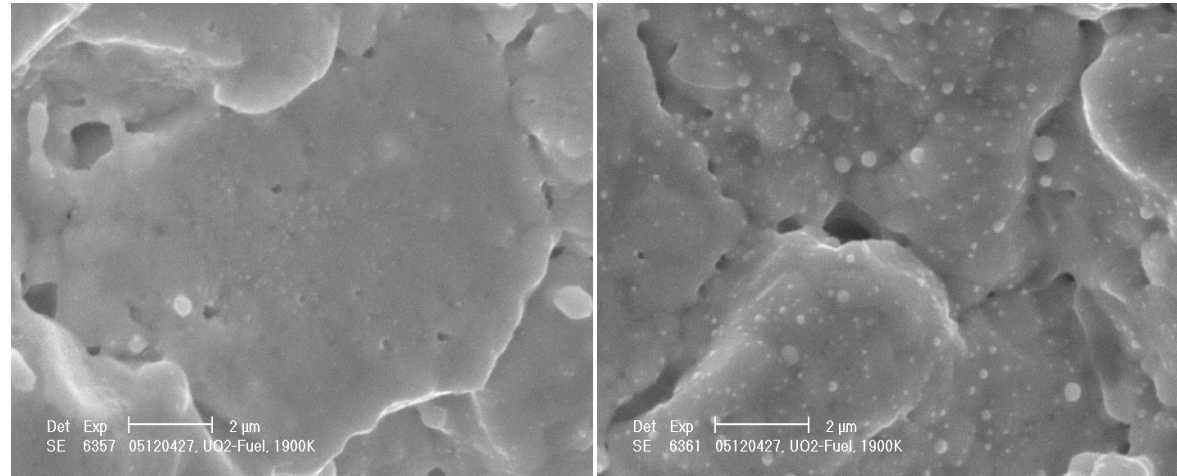


Knudsen cell – SEM analysis

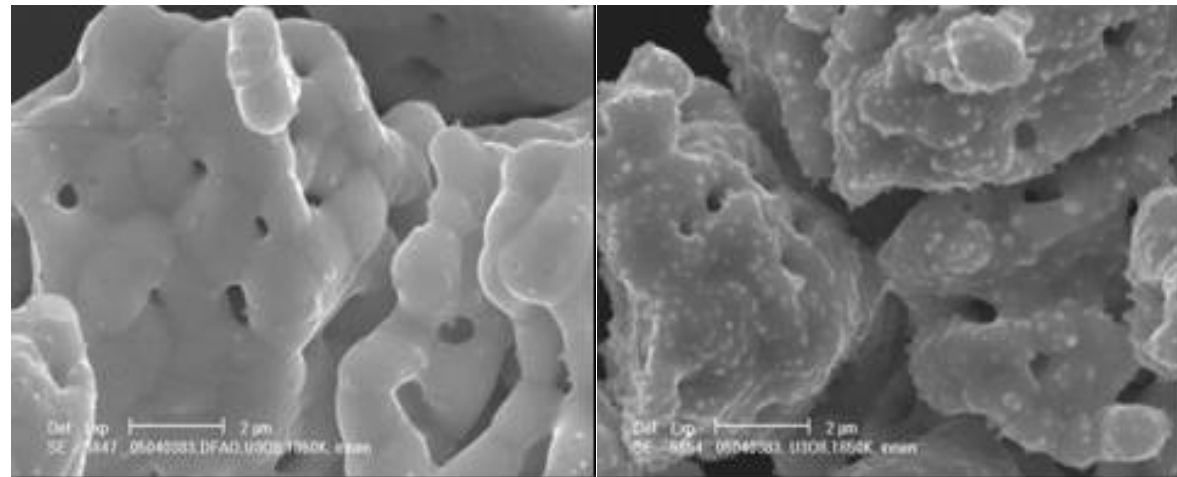


Annealed 1900 K in vacuum

oxidation effects



Annealed 1900 K preoxidized



outer surface

fracture surface

Lines of development for Knudsen cell



- the effects of burnup and of irradiation temperature on the *fg* **release behaviour in UO₂** have been characterized and modeled (rim structure effects)
- extension to **MOX** and irradiated **IMF/MX** fuels
- microstructural mechanisms responsible for property deterioration: **parallel micro- and macro-structural characterizations using several techniques**
- *fp*/fission *vs.* He/alpha decay damage
- effects of (e.g.) **oxidizing conditions** on the effusion behaviour
- **basic properties of actinide compounds**

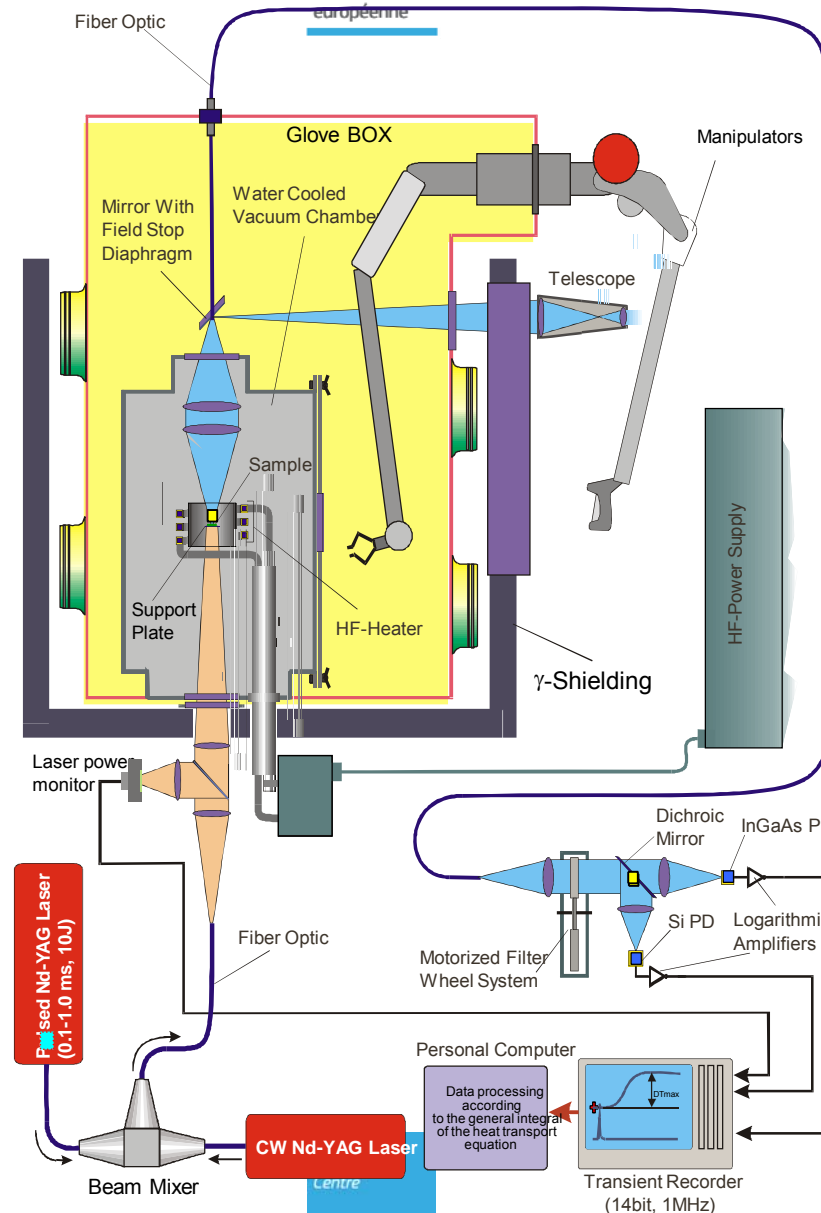
Laser flash apparatus



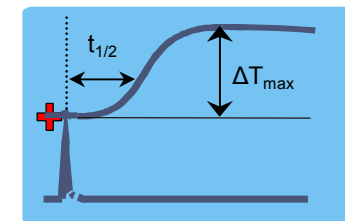
Commission européenne

sample subject to uniform T field
vacuum condition

1. HF induction furnace is heating up the sample.
2. when sample is at homogeneous T, laser shot is fired towards sample's front face.
3. the T wave generated by the laser shot moves through the sample towards the rear surface.



4. the heat front reaches the rear sample surface generating a T increase.
5. the increasing T thermogram measured by highly sensitive fast pyrometer.



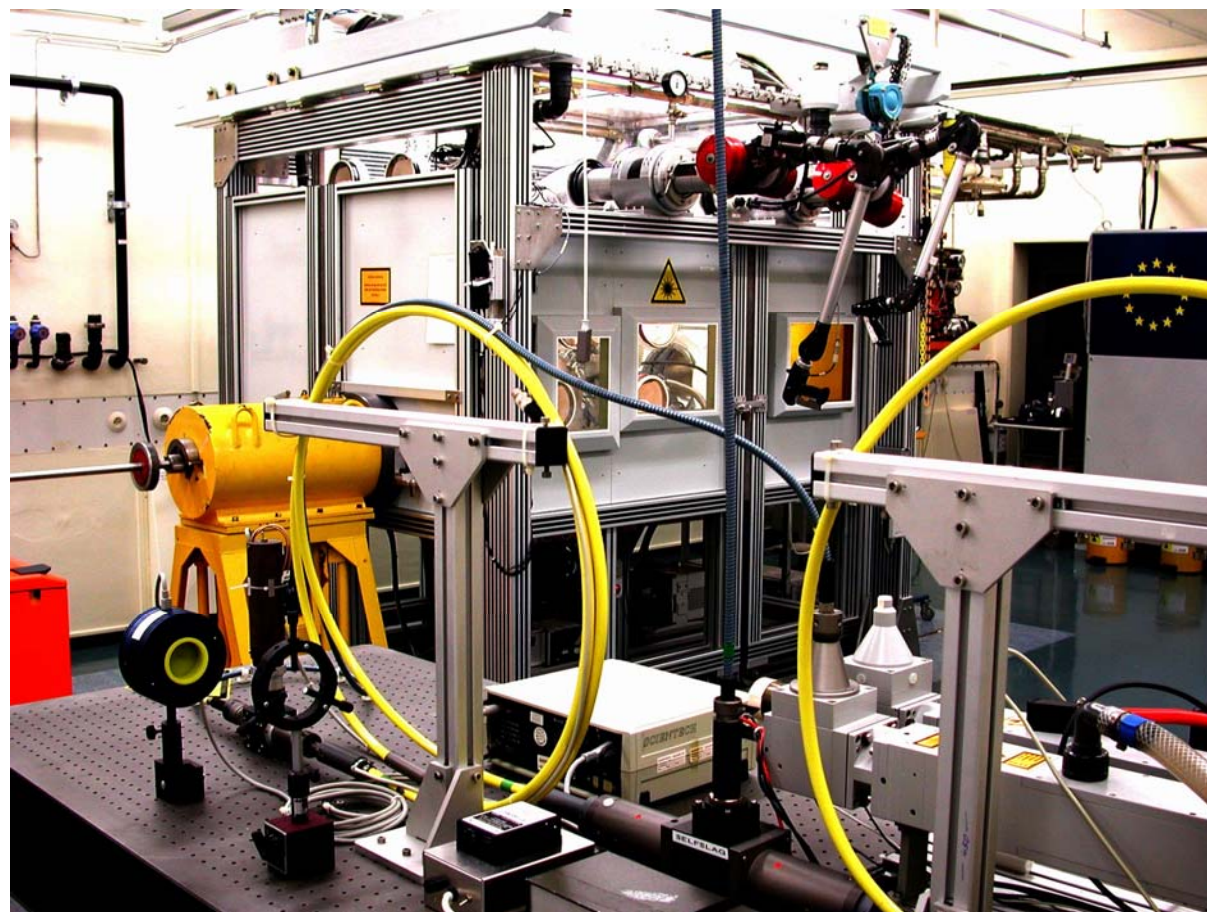
$$a = 0.13885 L^2/t_{1/2}$$

$$C_p = Q^*/\Delta T_{max}$$



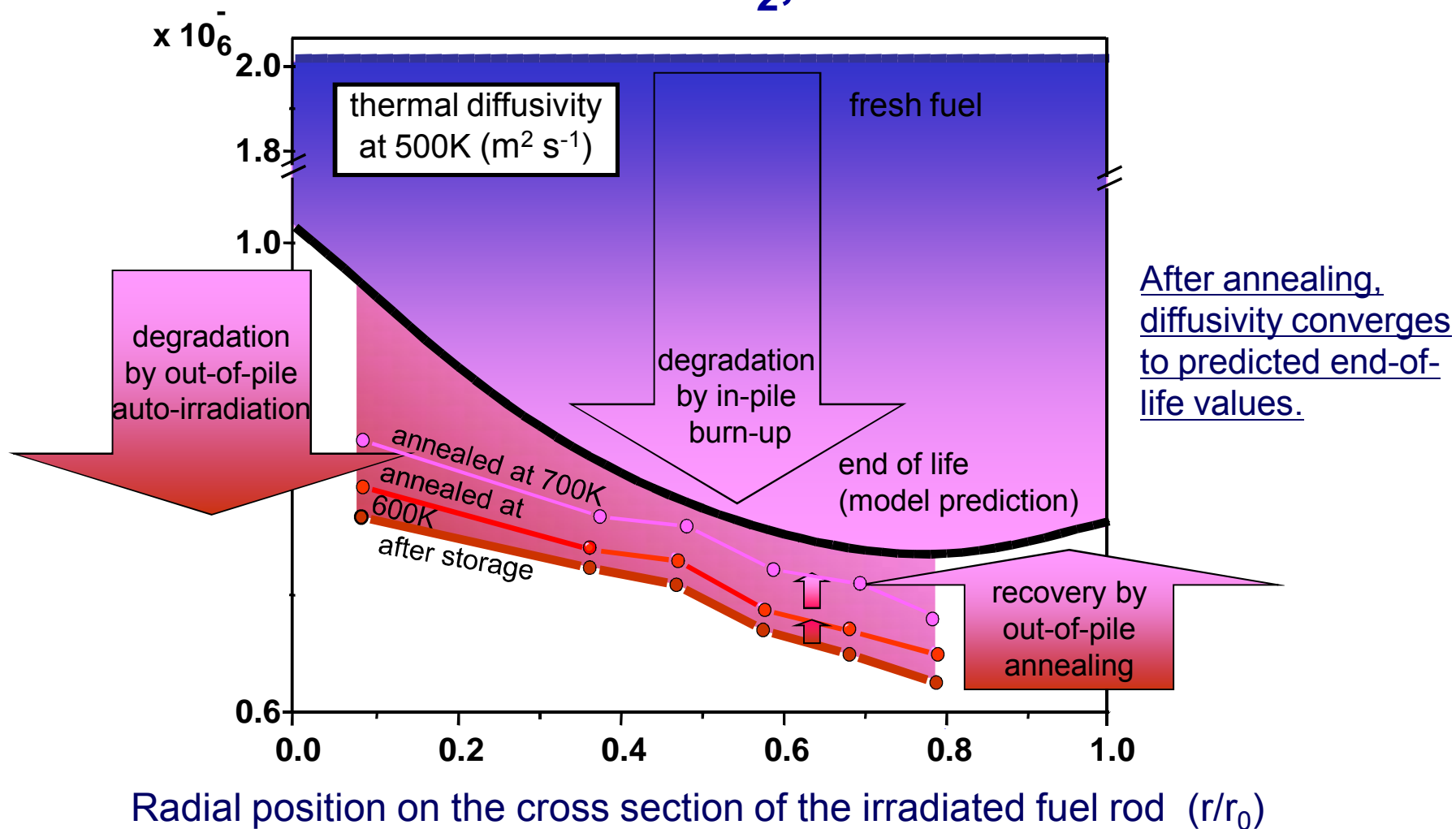
Commission
européenne

V



Joint
Research
Centre

Commercial UO₂, 100 GWd/t

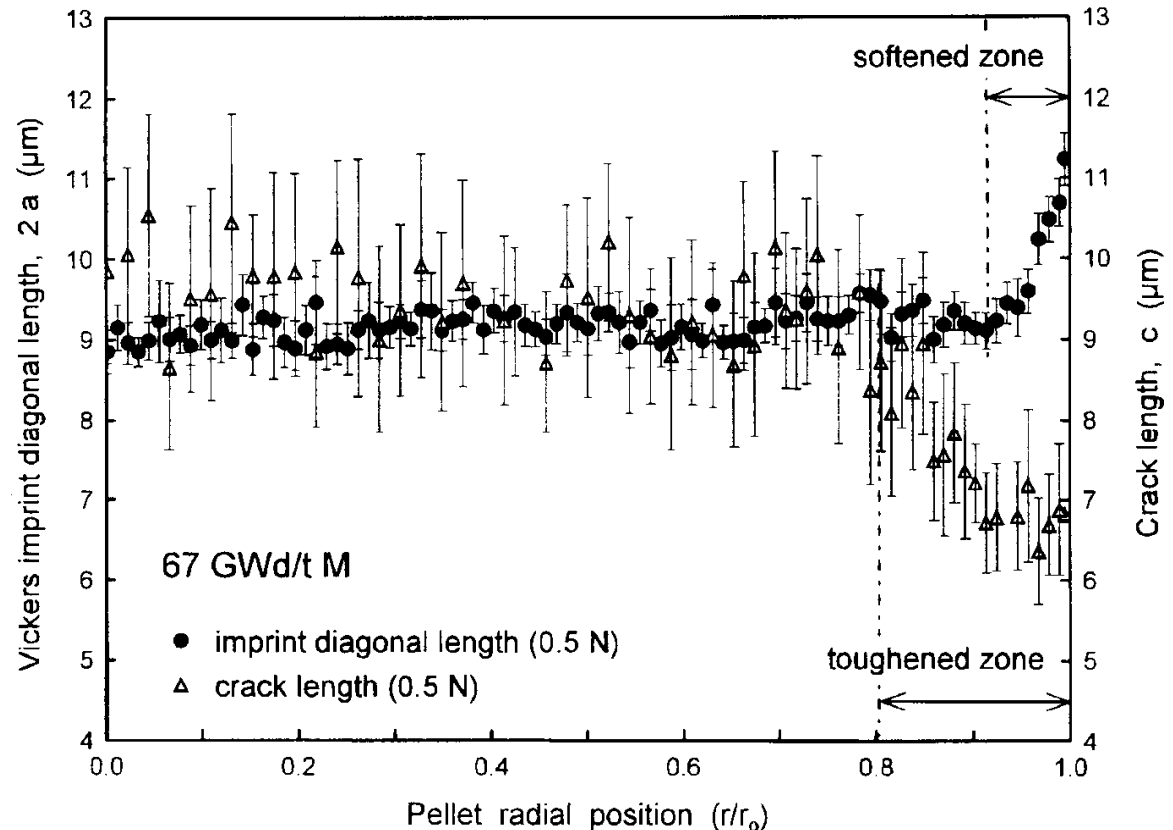


Mechanical behaviour of LWR fuel (microindentation)

Spino et al., 2003

LWR 67 GWd/tM,
indentation load 0.5 N

Radial profile of indentation:
Vickers print diagonal and
crack length as a function of
pellet radial position.

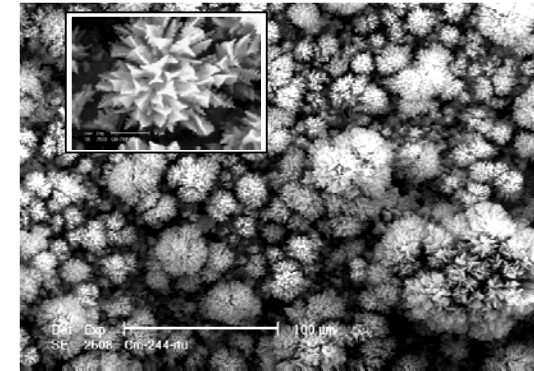


Softening at the rim corresponds to increased porosity due to the restructuring process

Negative effects of radiation damage, He accumulation on waste forms

- **amorphization:**
corrosion in water 20-50 times faster
(conditioning matrices)
- **swelling:** pressurization of clad/container
(spent fuel and conditioning matrices)
- **loss of mechanical integrity:**
surface area increase
(mainly spent fuel)

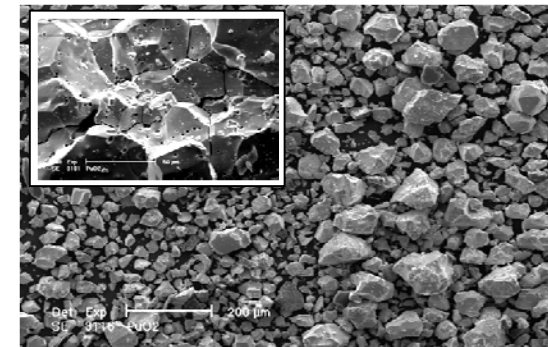
Surface structure



Sintered $^{244}\text{Cm}_2\text{O}_3$

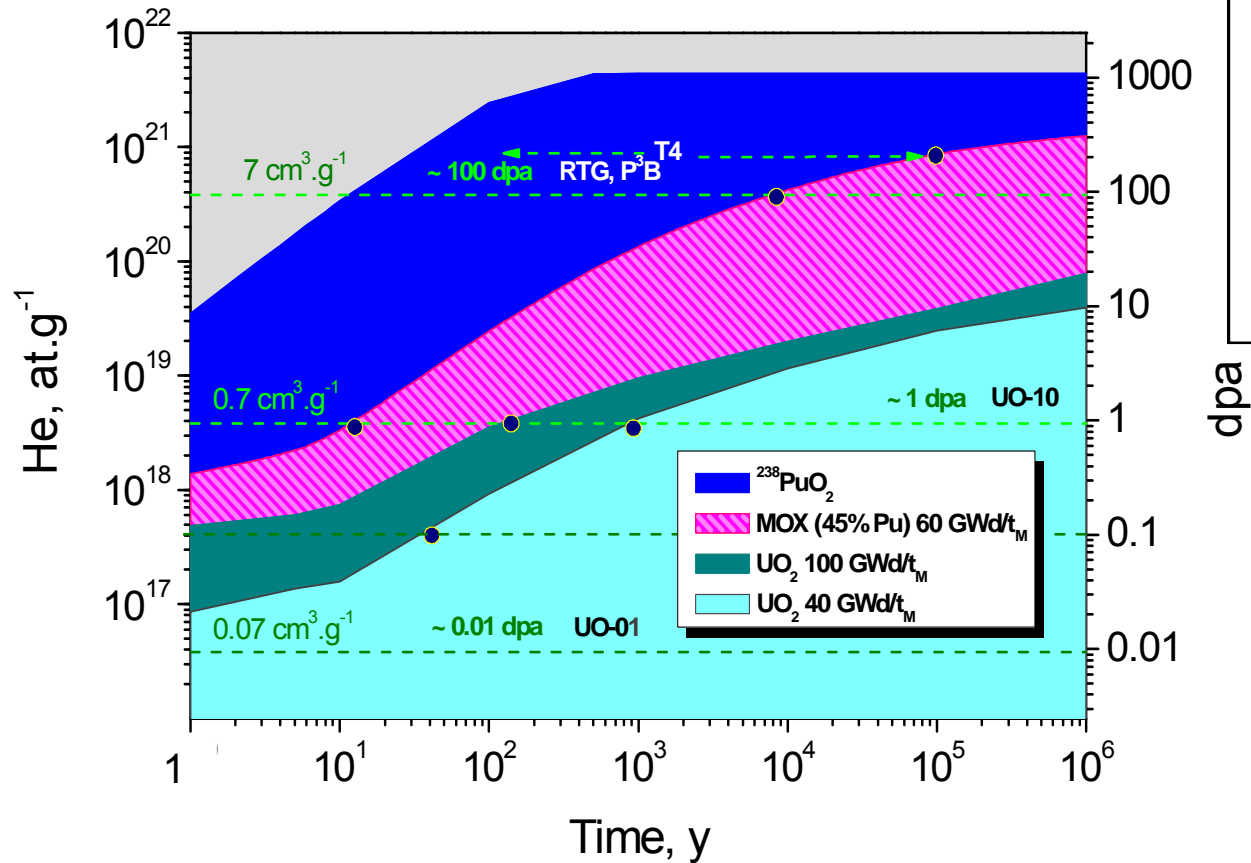
extreme consequences
after 35y at RT (uncontrolled)

Ceramographic



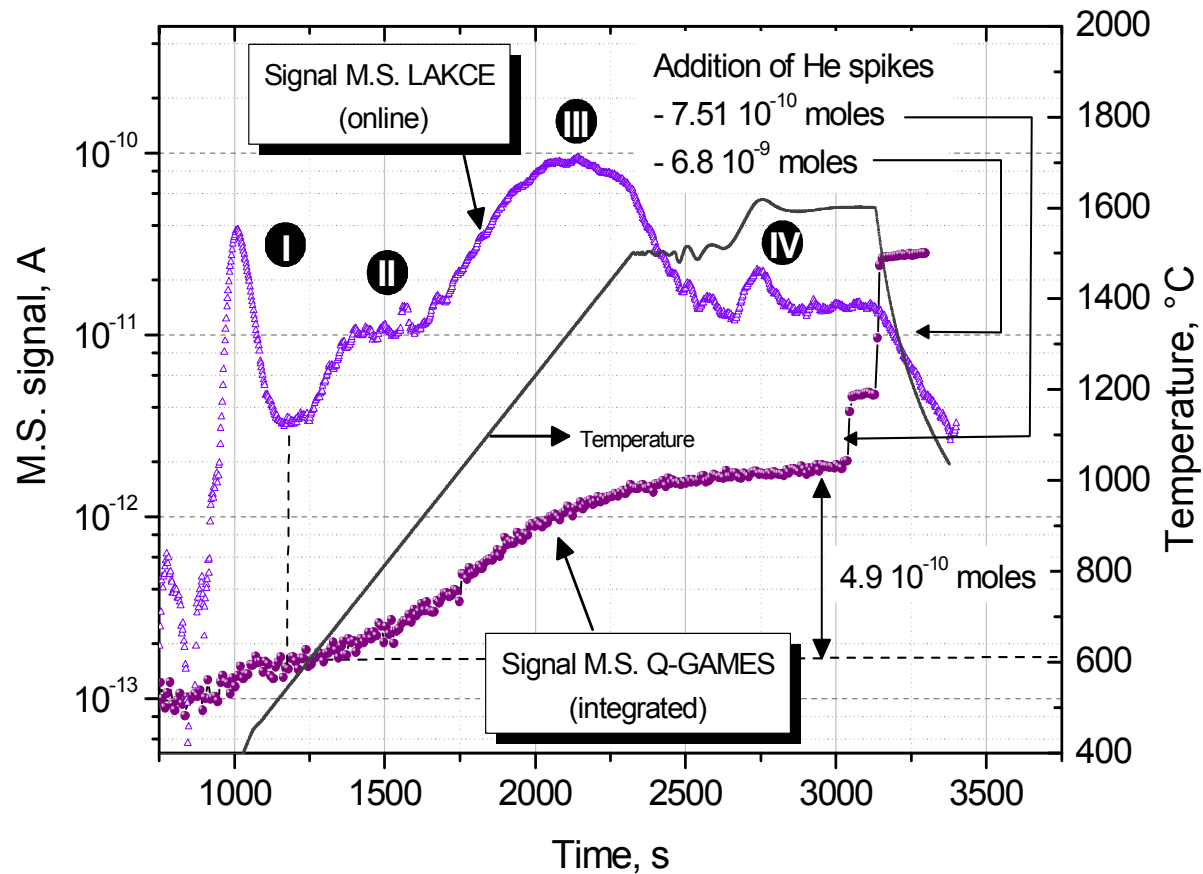
PuO_2 sintered pellet

Helium formation in nuclear fuels



Free volume in a rod: 20 cm³
 Pressure at EOI: 40 bar
 Hydrostatic P disposal: 50 bar
 Increase e.g. 50 bar
 - Pacemaker = MOX 8000 y

Helium solubility

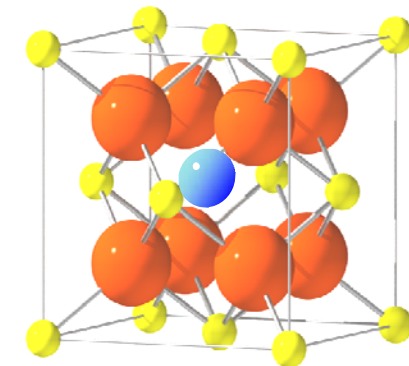
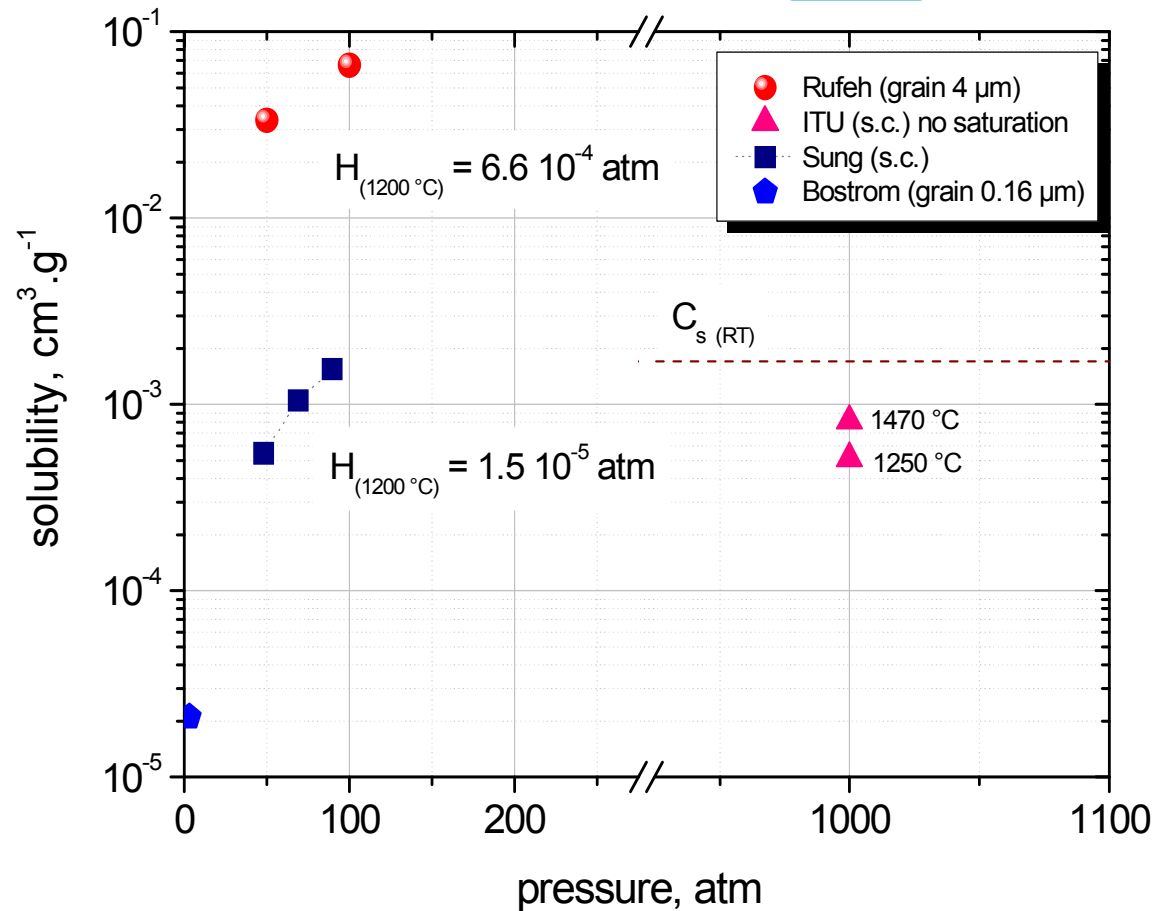


P = 1 kbar,
 T = 1250
 ° C
 t = 1 h

The solubility of He in UO_2 single crystal (for this operating conditions) is

$$2.29 \cdot 10^{-8} \text{ mol.g}^{-1} \quad (5.13 \cdot 10^{-4} \text{ cm}^3.\text{g}^{-1}).$$

Helium solubility



Helium radius: 31 pm

Octahedral site: 37 pm

Solubility follows Henry's law (limit).

Helium occupies octahedral sites of the fluorite structure.

Sample description – Main results

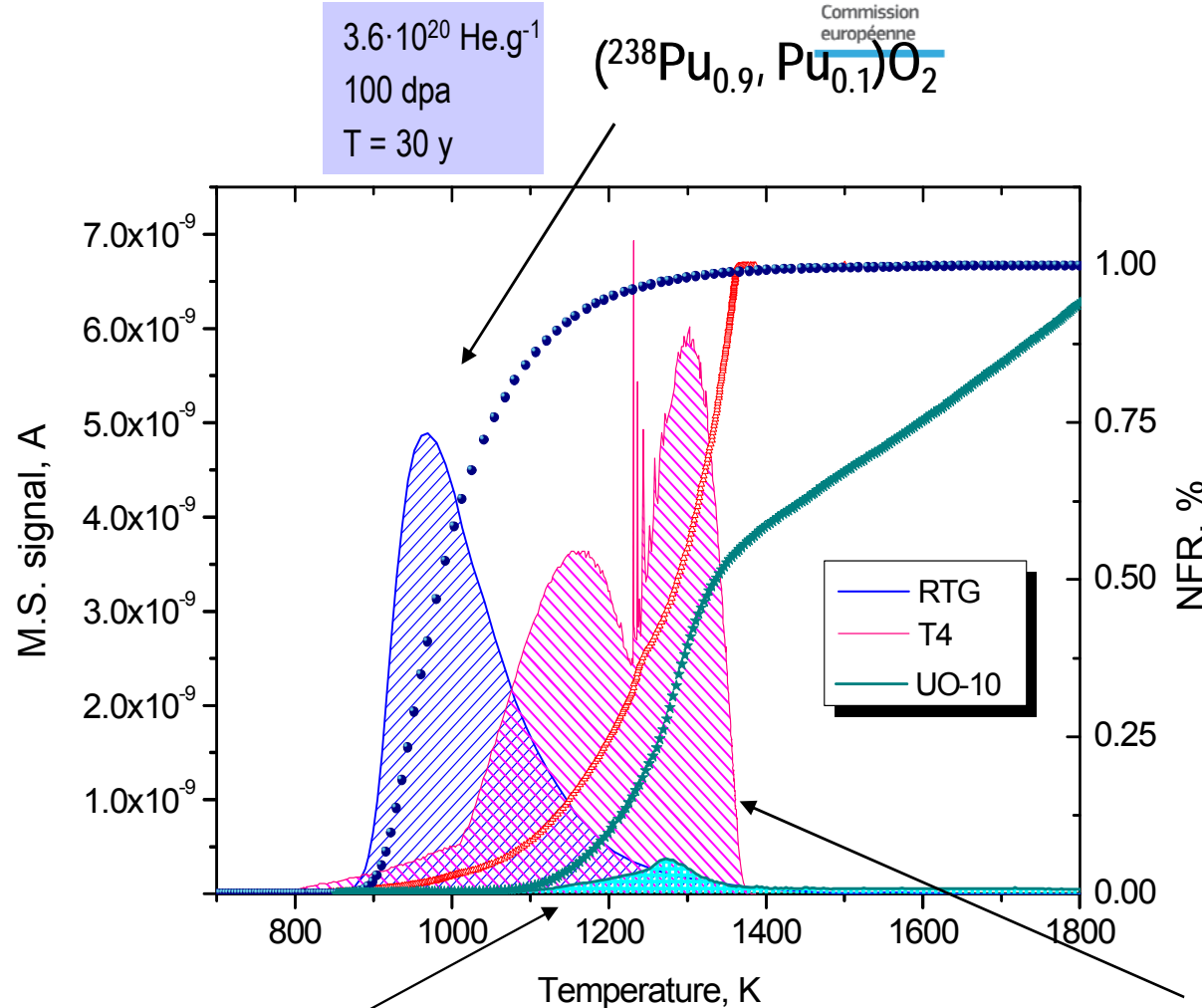
Commission
européenne

sample	Original composition	Age, y	Damage, dpa	He, at.g ⁻¹	Bubbles		Bubble pressure, MPa	Swelling, %	
					Average radius, nm	Conc., m ⁻³		lattice	From bubbles
UO233	(U _{0.9} ²³³ U _{0.1})O ₂	5	0.00001	3.8x10 ¹⁴				0.09	
UO01	(U _{0.999} ²³⁸ Pu _{0.001})O ₂	9	0.028	7.6x10 ¹⁶				0.5	
MOX40	(U _{0.6} ²³⁹ Pu _{0.4})O ₂	12	0.12	4.7x10 ¹⁷				0.7	
UO10	(U _{0.9} ²³⁸ Pu _{0.1})O ₂	9	2.8	7.6x10 ¹⁸	1.2	1.5x10²²		1.3	0.01
P ³ B	(²³⁸ Pu _{0.9} , Pu _{0.1})O ₂	30	100	3.6x10 ²⁰	2.5	5x10²³	180	2.2	3
RTG	²³⁸ PuO ₂	36	110	5.5x10 ²⁰					
T4	(U _{0.33} , Th _{0.67})O _{2+y}	550x10 ⁶	170	7.2x10 ²⁰	3	8x10²³	320	1.5	9
U2	(U _{0.92} , Th _{0.08})O _{2+y}	220 x10 ⁶	130	5.8x10 ²⁰				1.5	

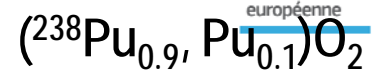
Nb: the van der Waals equation of state has not been used to calculate P_{bubble}

Joint
Research
Centre

He desorption from different systems



$3.6 \cdot 10^{20} \text{ He.g}^{-1}$
 100 dpa
 $T = 30 \text{ y}$



Commission européenne

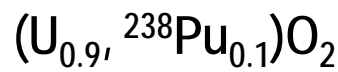
Fast kinetic :

- higher damage
- low release T

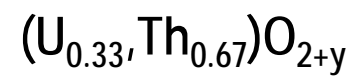
Low kinetic

- damage annealing
- high release T

$1.7 \cdot 10^{18} \text{ He.g}^{-1}$
 0.7 dpa
 $T = 2 \text{ y}$



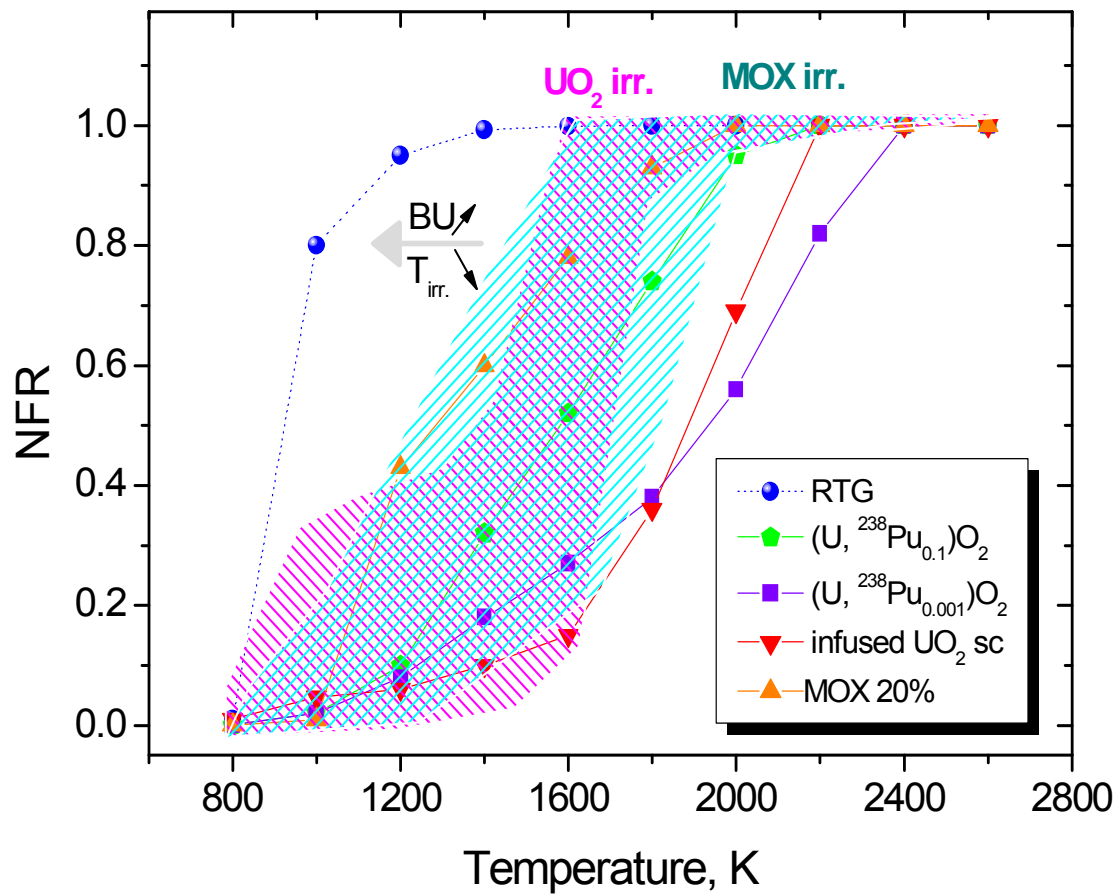
$7.2 \cdot 10^{20} \text{ He.g}^{-1}$
 170 dpa
 $T = 550 \cdot 10^6 \text{ y}$



Joint Research Centre



He-release from different systems



Factors affecting the release temperature:

- Burnup
- Oxydation
- Irradiation temperature
- alpha-damage
- He content

Measurement of the Specific Heat by Differential Scanning Calorimetry (DSC)



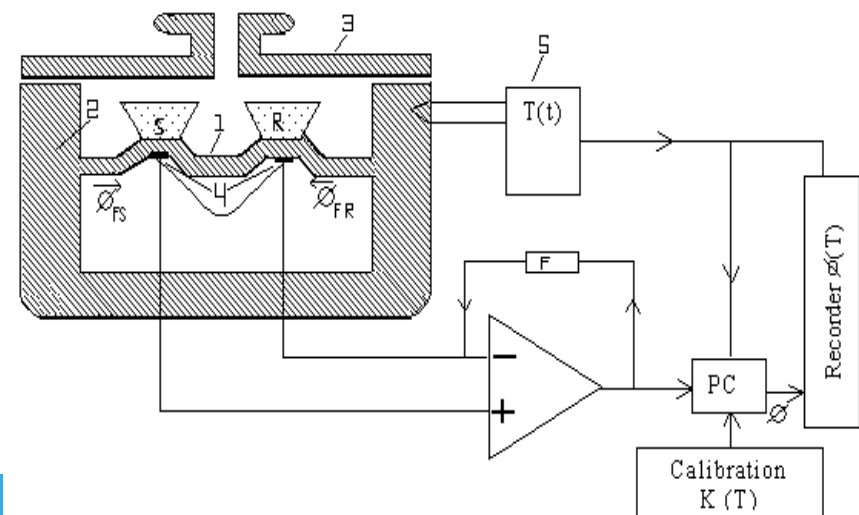
Thermal Analyzer **Netzsch STA 409**

Specific Heat for active samples

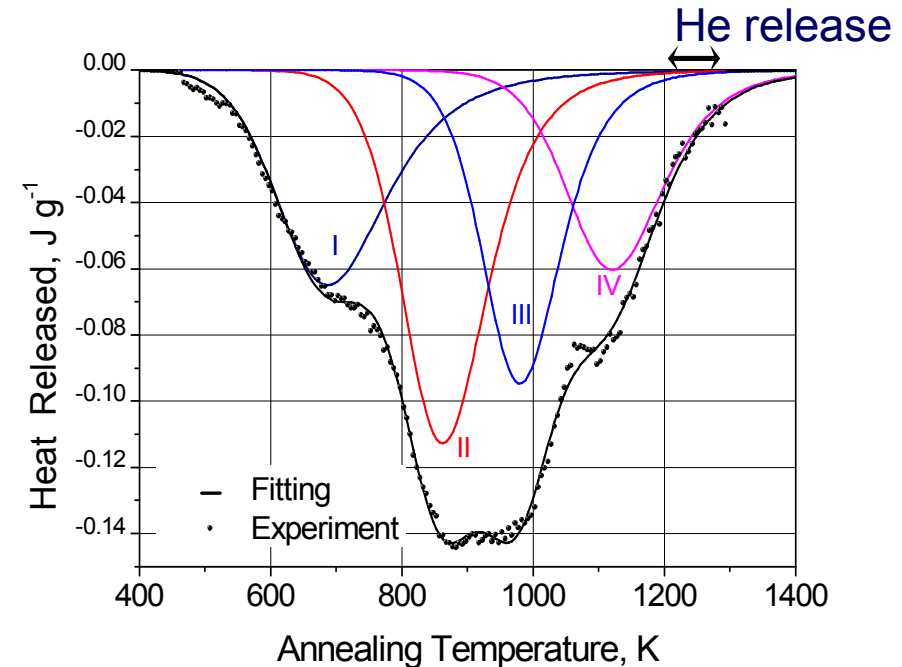
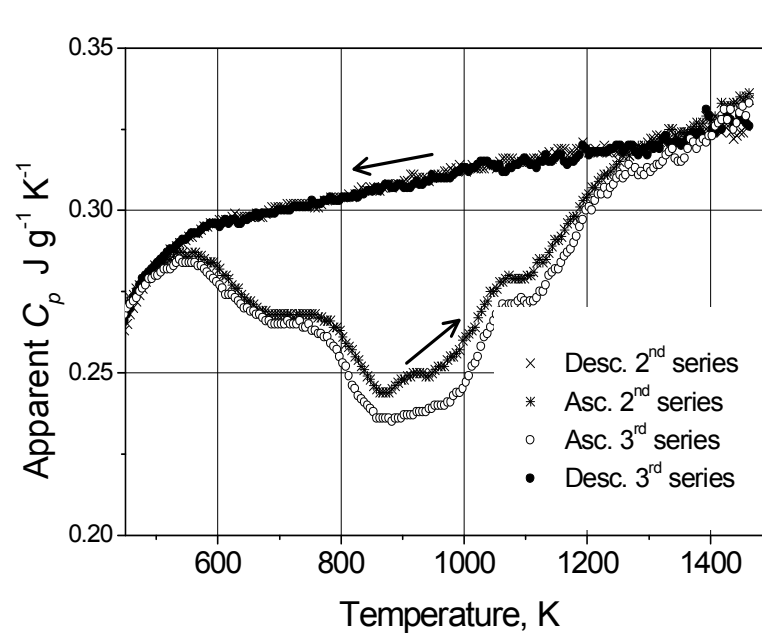
Heat effects associated to the annealing of radiation
damage

Sapphire reference sample (standard)

The characteristic feature of this measuring system is that the main heat flow from the furnace to the samples passes symmetrically through a disk of good thermal conductivity, (see Fig. 27).



Apparent C_p during annealing



Reproducible runs after 5 and 6 months storage ($15 K min^{-1}$).

The deviation of initial $C_p^*(T)$ from annealed $C_p(T)$ is due to recovery of latent heat of lattice defects. Curves corrected for the α -decay heat ($\sim 0.14 J g^{-1} K^{-1}$)

Heat effects

- I : O vacancy-interstitial recombination (14 J/g)
- II : U vacancy-interstitial recombination (19 J/g)
- III : Loop annealing (12 J/g)
- IV : Void precipitation (15 J/g)

Thermal conductivity $\lambda = (A + BT)^{-1}$



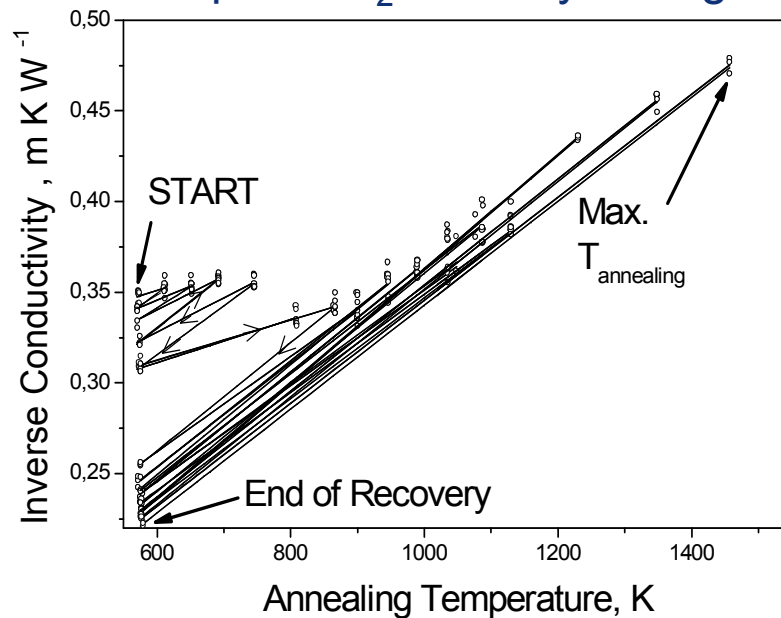
A accounts for phonon-impurity scattering due to point defects [$f(T)$, saturation]

B should account for variation of the elastic properties with increasing damage:

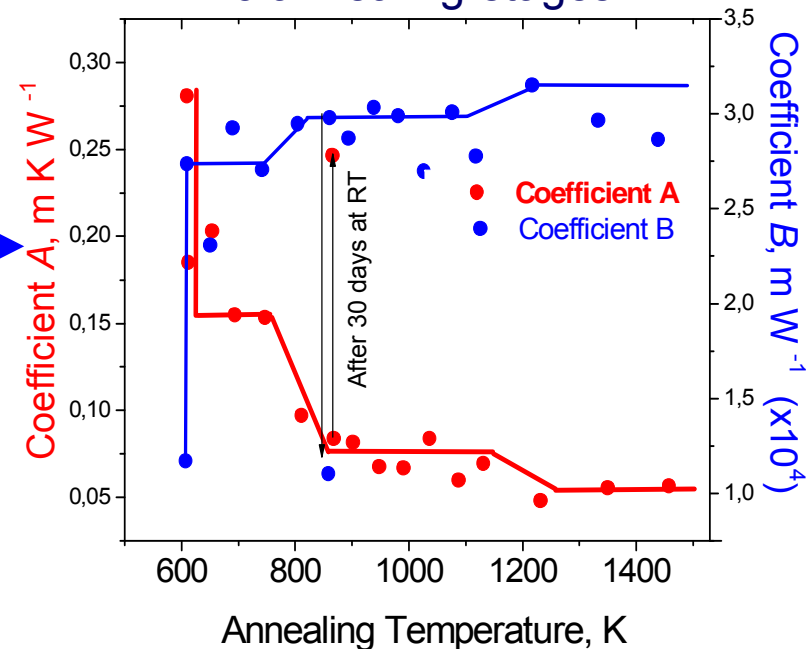
effect of thermal annealing: decrease of A and increase of B

λ degradation does not depend linearly on the concentration of defects, saturation occurs early; thermal recovery of λ can be used only to determine T ranges for healing.

α -doped UO_2 after 5 y storage



3 annealing stages



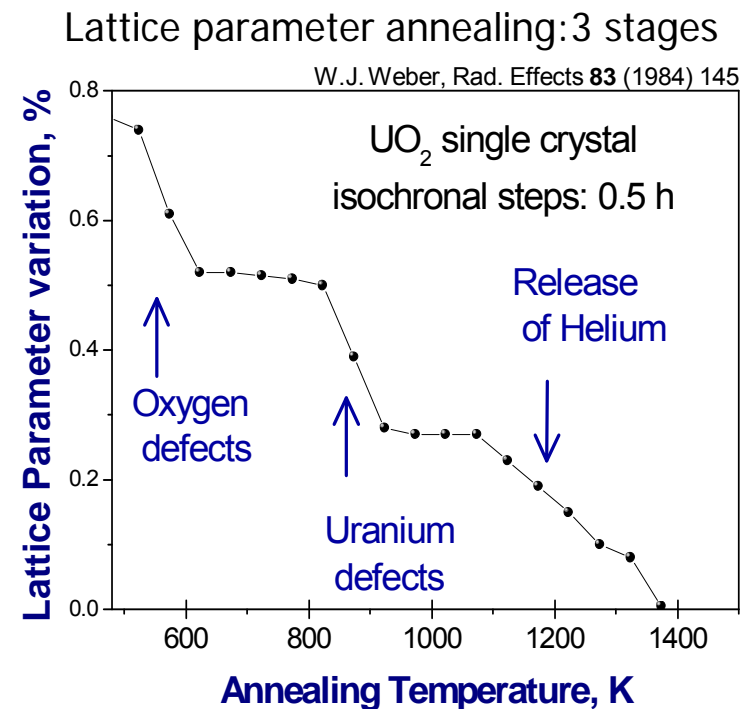
Annealing of microstructural defects



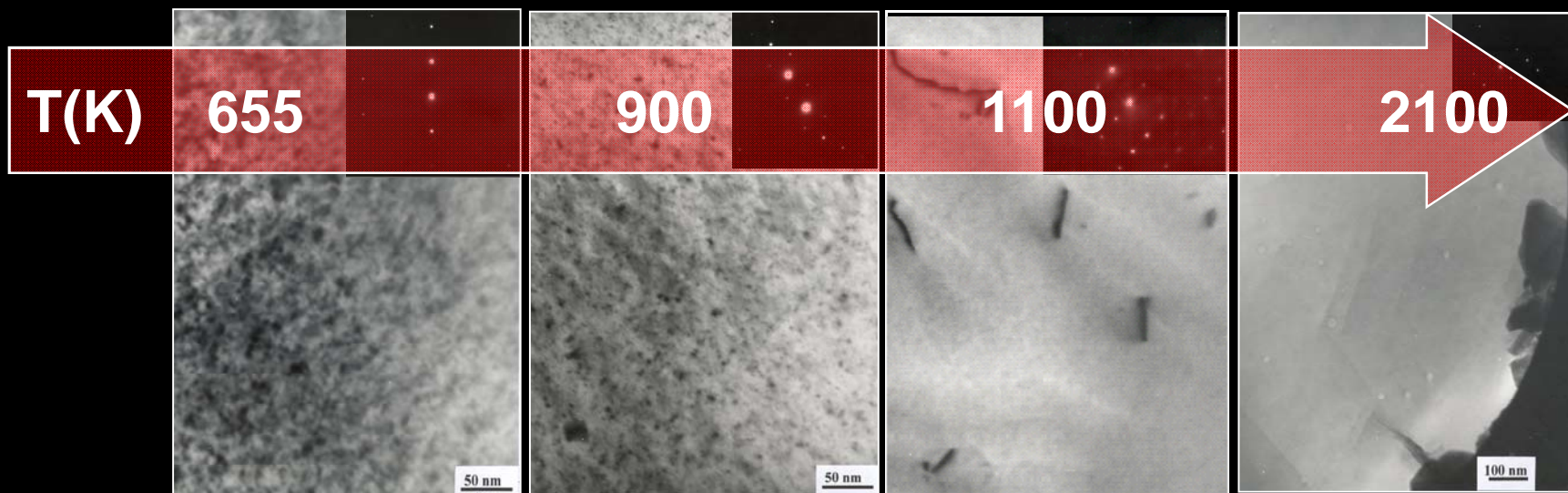
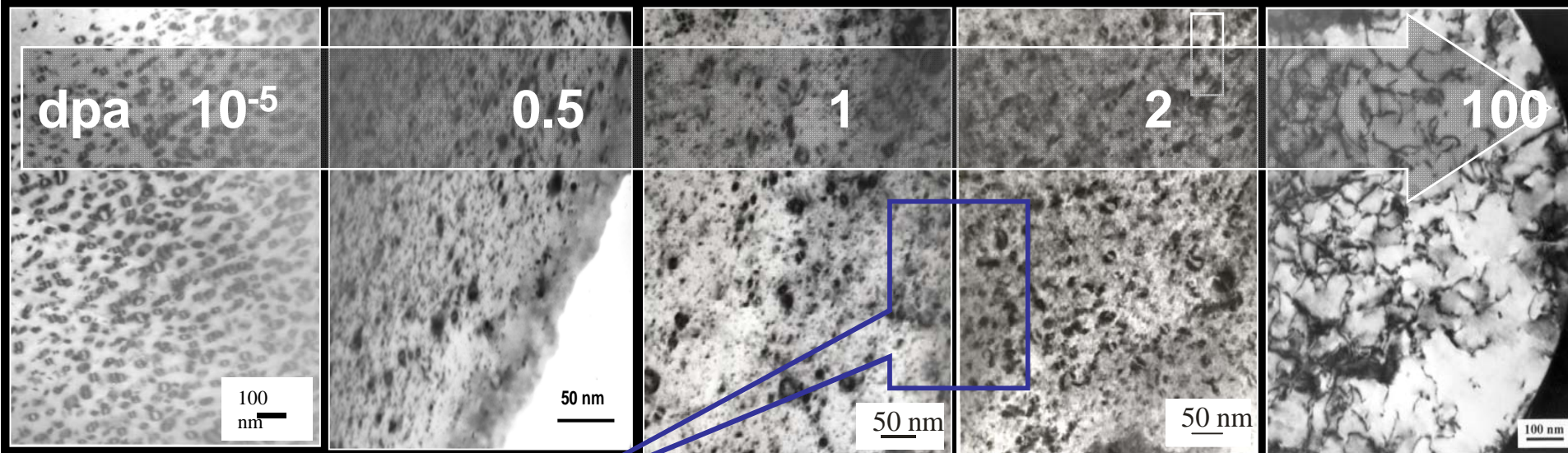
Combined analysis of independent recovery processes:

- microstructure (void/dislocation)
- calorimetry
- He release
- thermal conductivity
- lattice parameter

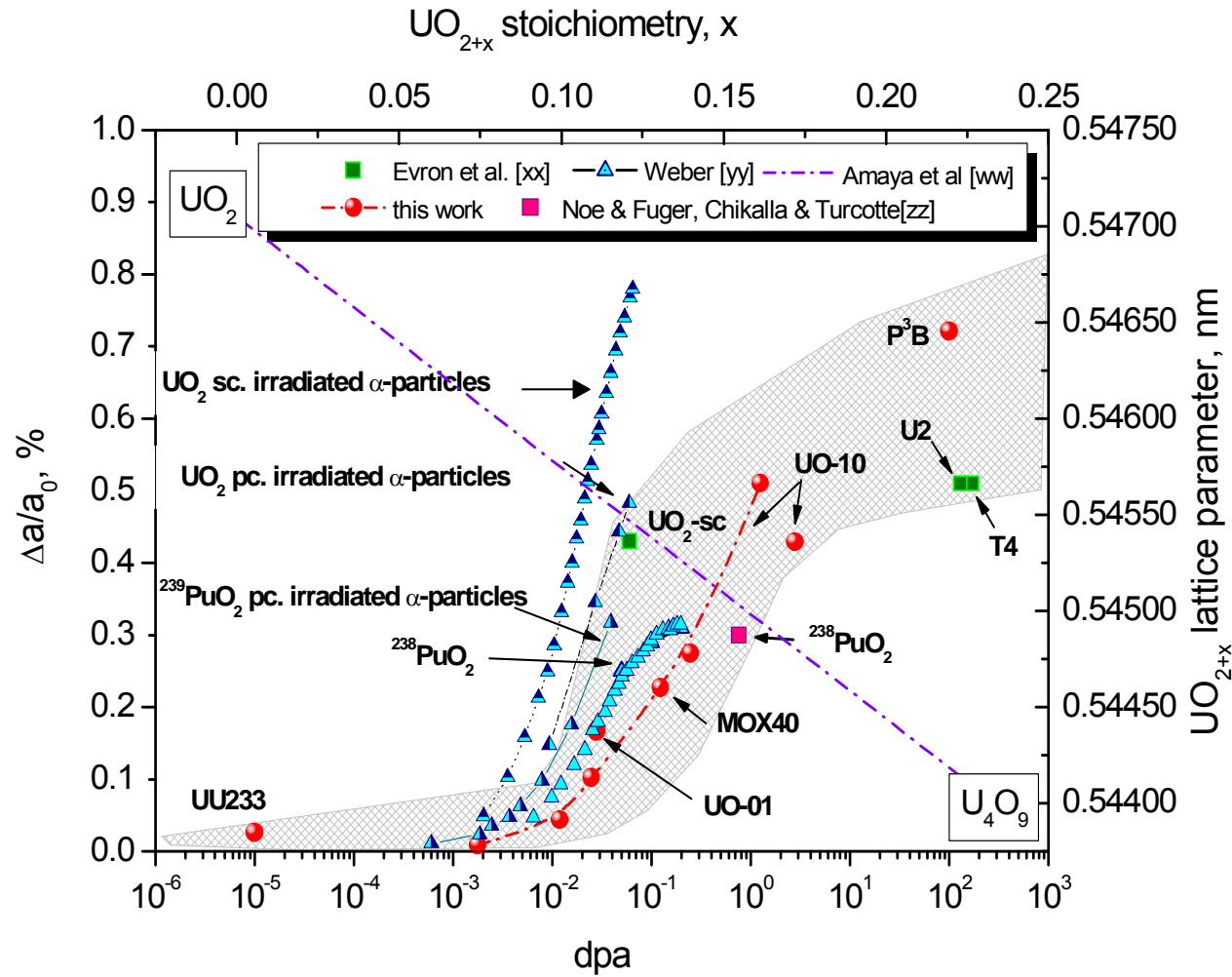
- ✓ concentration of defects:
 - microstructure examination
 - lattice parameter changes
- ✓ determination of temperature stages
- ✓ energy associated with defects (apparent C_p)



TEM alpha-damaged $(U_x, Pu_{1-x})O_2$

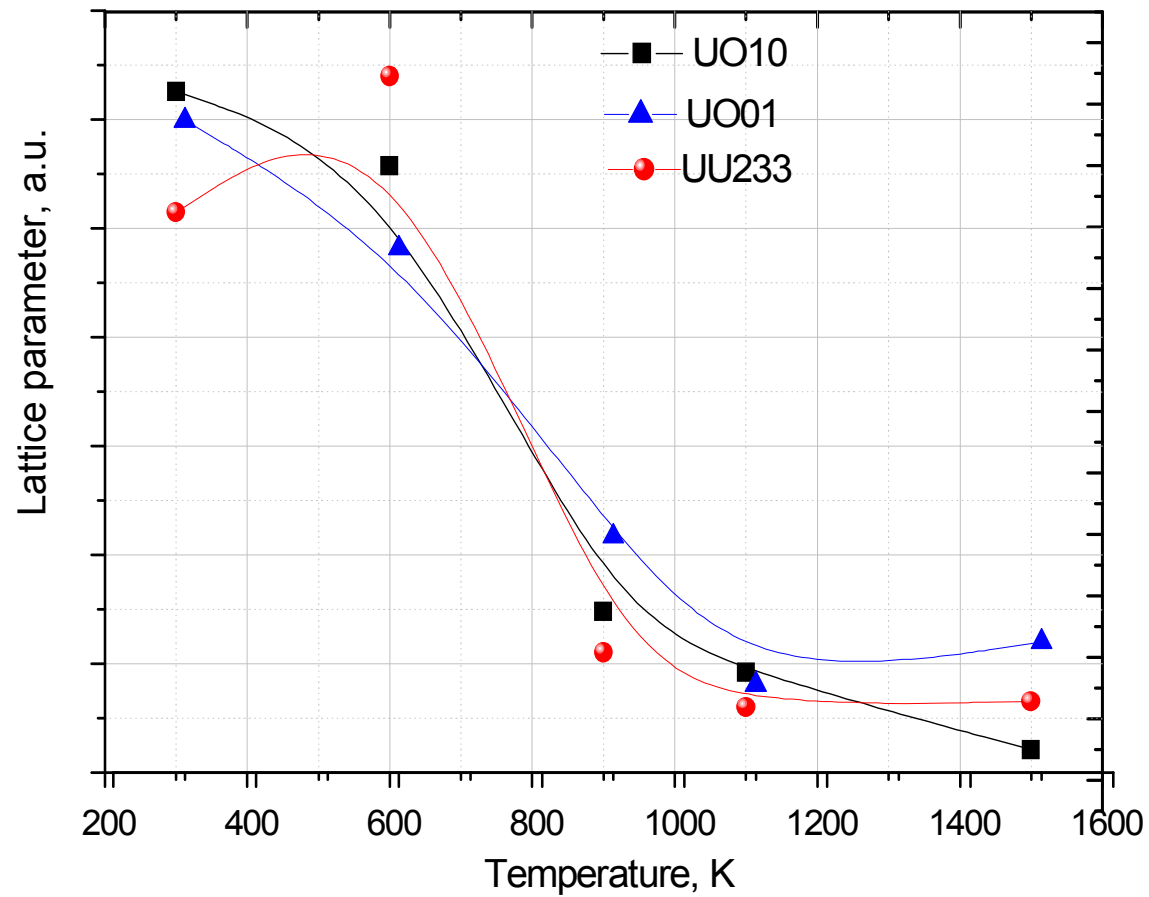


XRD analysis of α -damaged samples



- Oxidation \downarrow
- Damage \uparrow
- Kinetic effects
- Saturation

XRD annealing of alpha-doped UO_2



Representativeness of accelerated damage

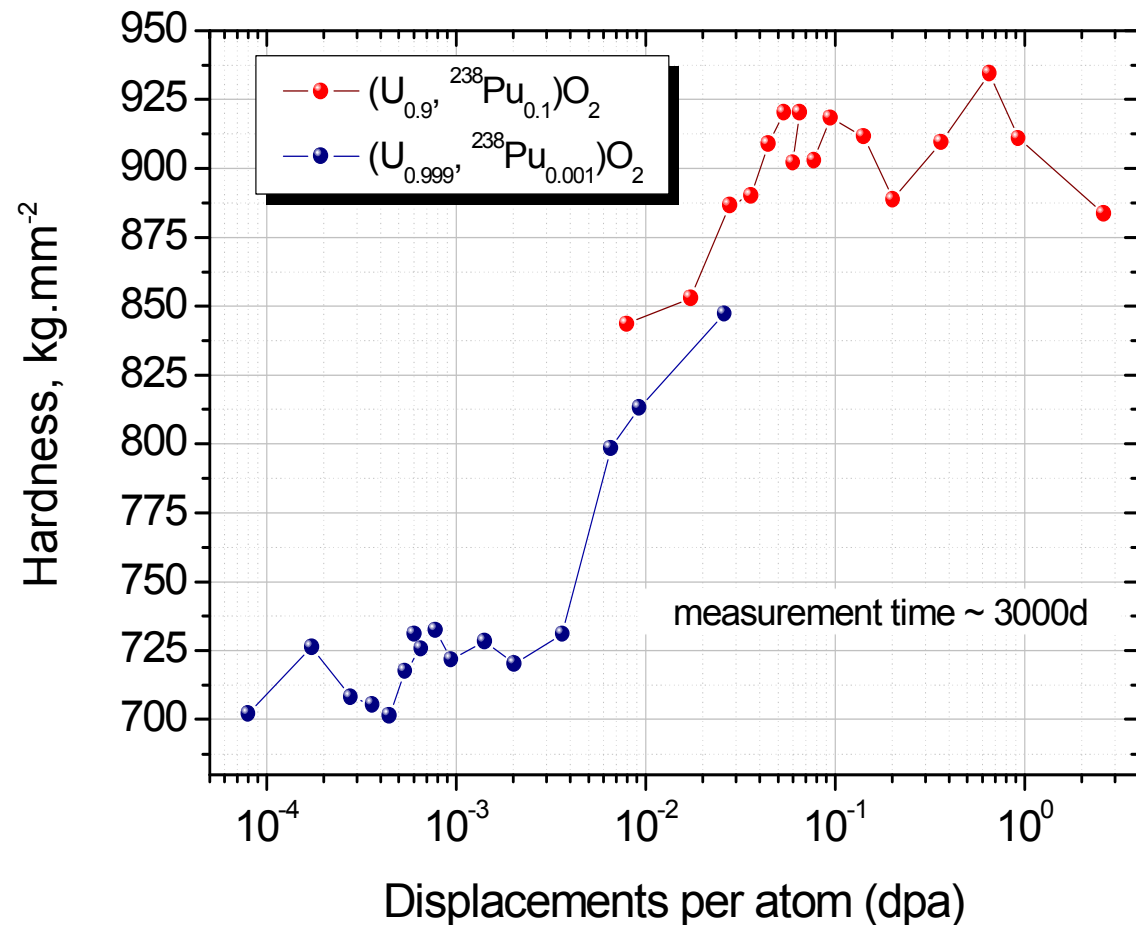


hardness vs. damage

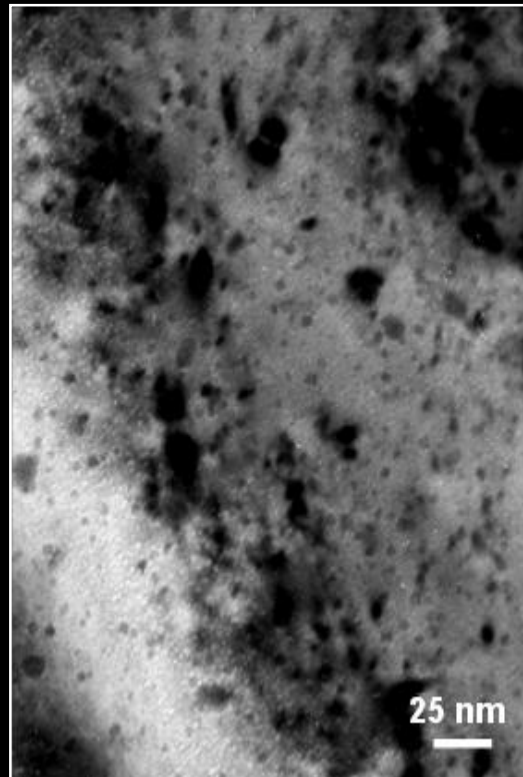
The evolution of hardness for these materials is determined by accumulated damage and not affected by composition.

The dose rate does not affect the property evolution in this range of alpha-activities.

Accelerated damage accumulation is representative of aging process



TEM analysis of $(U_x, Th_y, Pu_z)O_2$



$1.7 \cdot 10^{18} \text{ He.g}^{-1}$

0.7 dpa

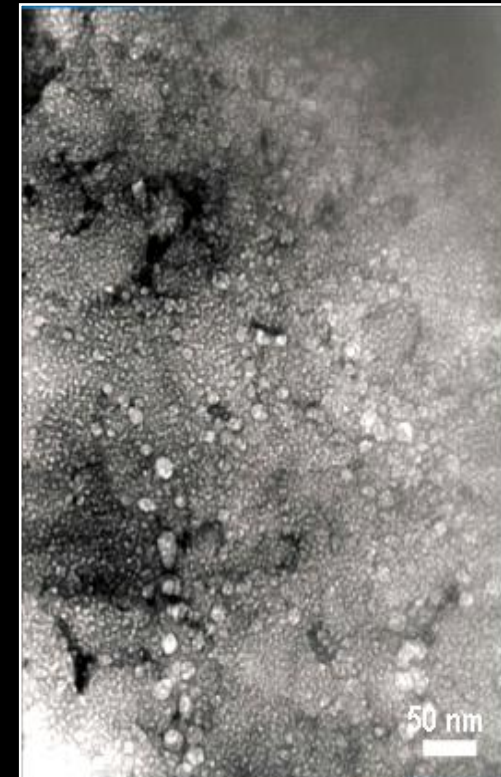
T = 2 y



$3.6 \cdot 10^{20} \text{ He.g}^{-1}$

100 dpa

T = 30 y



$7.2 \cdot 10^{20} \text{ He.g}^{-1}$

170 dpa

T = $550 \cdot 10^6$ y

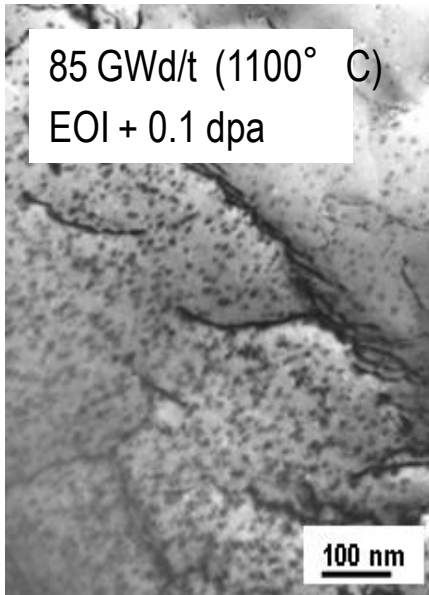


Alpha-damage in UO₂

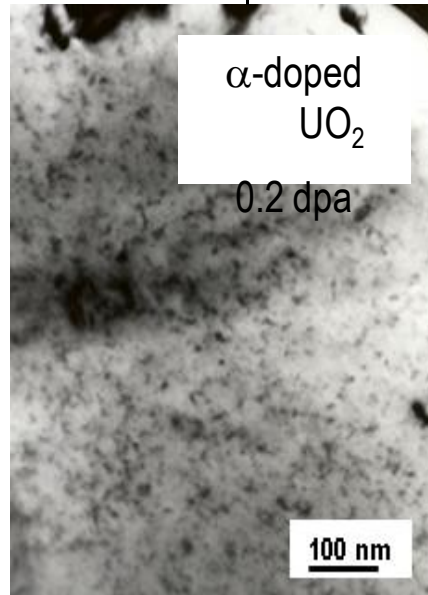


Commission européenne

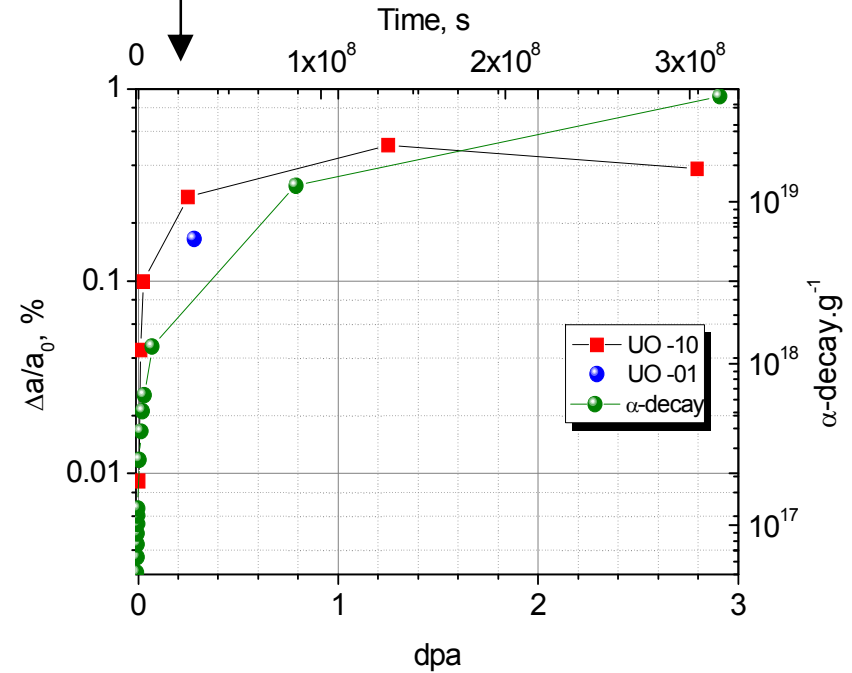
Large damage ingrowth



Irradiated fuel



(U_{0.9}, ²³⁸Pu_{0.1})O₂



PIE performed are affected by the growth of alpha-damage, even at low dose e.g. lattice parameter, thermal conductivity, microstructure

Conclusion / perspectives



- Rapid lattice swelling and saturation at $\sim 2\%$
 - consequence of extended defects ingrowth (polygonisation?)
- Low helium solubility ($\sim 2\%$ MOX fuel)
 - verify the limit of Henry's law
- Gas swelling between 3 and 9 % !
 - assess the fraction retained (i.e. pressure in the bubbles using van der Waals equation of state)
- Probable embrittlement/disintegration of the fuel
 - fracture stress and bubble pressure
- Extrapolation to behaviour of fuel during short time storage
- Basic aspects on helium behaviour – alpha-damage (GEN IV)

Conclusions



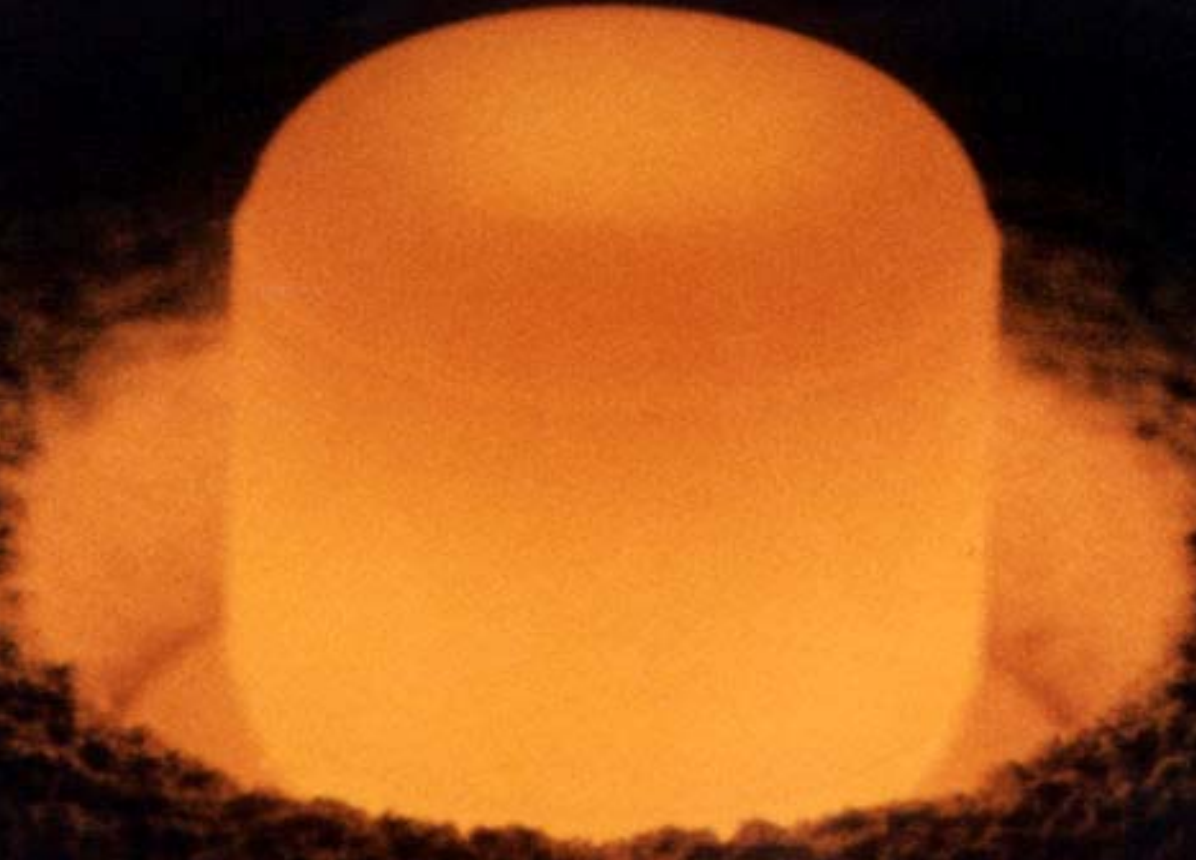
- Combined analyses allowed quantification of damage and recovery process.
- Accelerated decay accumulation was validated as representative of long-term ageing of high-level waste forms.
- Comparison with irradiated fuels shows that damage effects and recovery processes during thermal annealing occur by similar mechanisms in α - and fission-damaged UO_2 : → towards a unified understanding of radiation damage.

The High Burnup Structure (HBS)



- HBS (or RIM) structure is formed at high local burnup and low T_{irr} . It is characterized by grain subdivision, increased porosity, and evolves to an “ultimate” microstructure at very high burnup.
- No universal consensus on mechanisms and properties of HBS.
- However, it seems that HBS is not a negative feature of high burnup fuel:
 - fg is not released when HBS is formed
 - depletion of fission gases in the matrix, but almost complete retention in the fuel (rim porosity).
 - but release temperature decreases with decreasing T_{irr} and increasing burnup

Aknowledgements

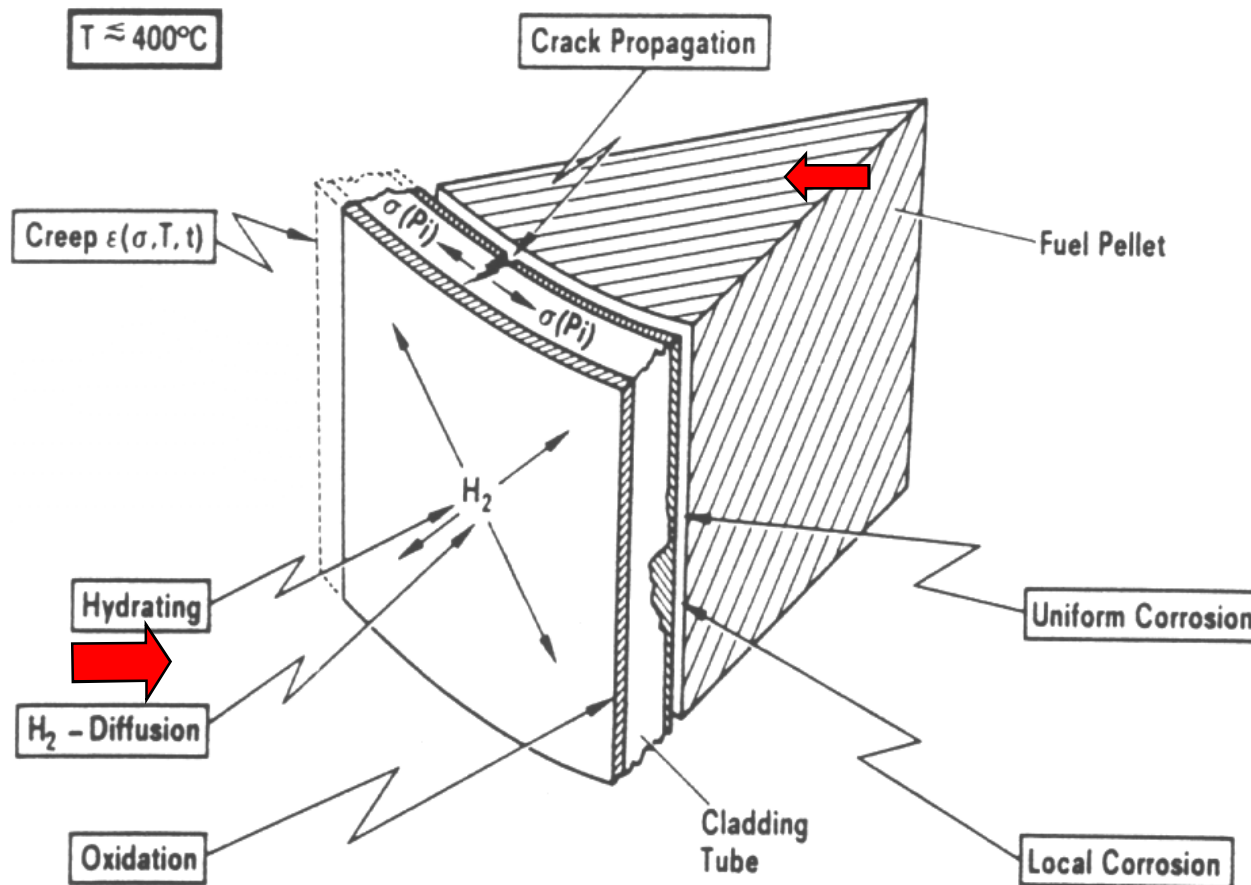


V. Rondinella, Hj. Matzke, R. Konings, J.-P. Hiernaut, H. Thiele, J.-Y. Colle, B. Cremer, R. Jardin, D. Bouxière, J. Cobos (ITU), R. Conrad (IE), N. Chauvin, J. Noirot, D. Roudil, X. Deschanel, P. Garcia (CEA), C. Thiriet-Dodane, P. Lucuta (AECL), W. Weber (PNNL), R. Schramm, F. Klaassen, K. Bakker (NRG), A. van Veen (IRI), AREVA, CRIEPI, GSI, GANIL

Cladding



Cladding behaviour during storage (and transport)



Cladding



Segmented Cone Mandrel Test

Displacement controlled
→ stable crack growth

“cold” development in IE

optimization and implementation in hot cell in
ITU for application on irradiated cladding

extending existing creep test capabilities



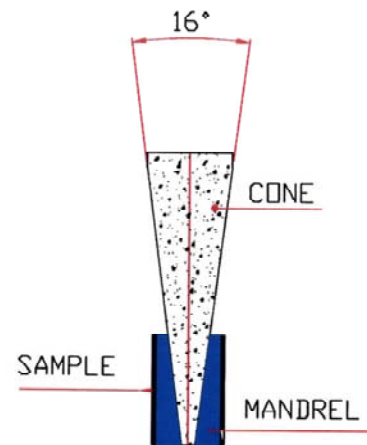
Cladding



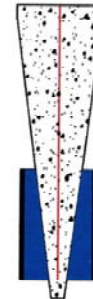
Commission
européenne

Schematics of SCMT Design

ITU - Prototype (Cone/Mandrel - Concept)



Starting position



LOW DEFORMATION (5%)
(Interim Storage / RIA-case)



HIGH DEFORMATION (50%)
(LOCA-case)

Localise deformation
(Finite Elements calibration needed)

Crack detection measurement on fuel cladding based on eddy current

*V.V. Rondinella, D. Papaioannou, J. Ejton,
W. de Weerd, R. Nasyrow, H. Toscano, W. Goll**

** AREVA NP GmbH, FDEEM, Erlangen, Germany*

Manual (dynamic) crack detection; small surface cracks on high-alloyed in unspecified locations (independent of the direction of the inspection).

PROBE SYSTEM: Absolute, ferrite core, transformer

FREQUENCY RANGE: 100 kHz - 3 MHz

ACTIVE AREA: Approx. 1.0 mm

PENETRATION DEPTH: Low

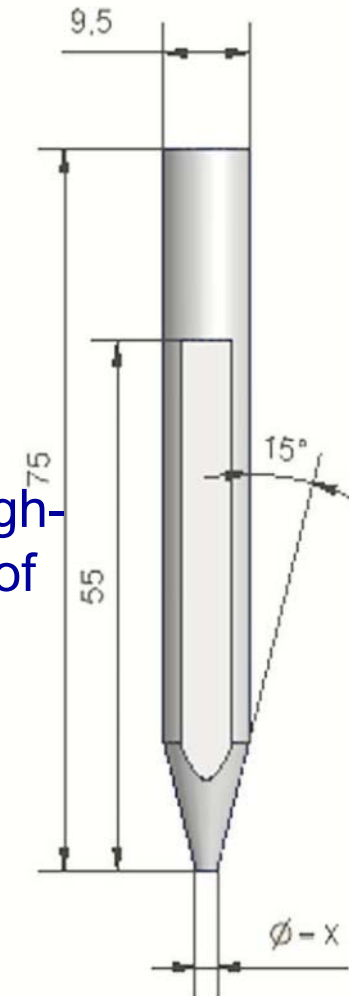
CABLE: EK-X-HF/1, EK-X-007

HOUSING: Plastics (Delrin); pencil housing # 2

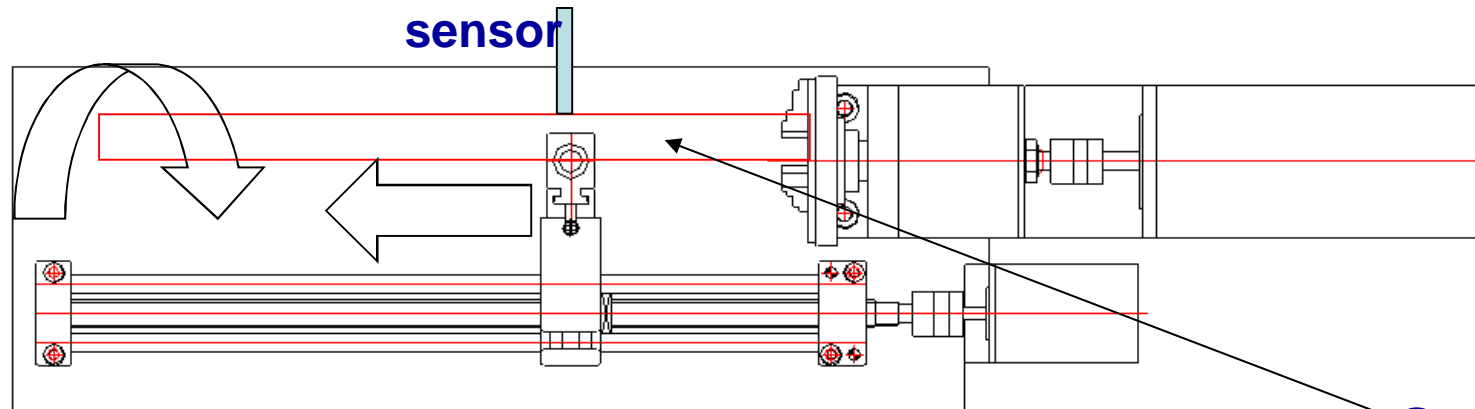
DIAMETER: 9.5 mm

LENGTH: 75.0 mm

WEIGHT: 10 g



Crack detection device

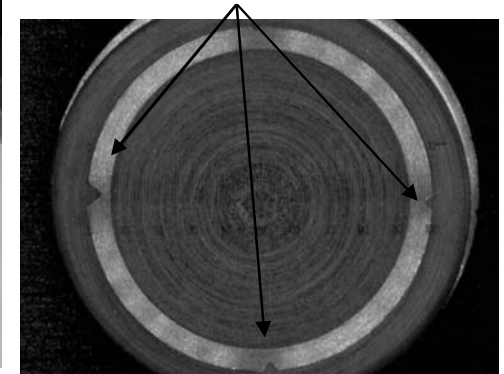


sensor

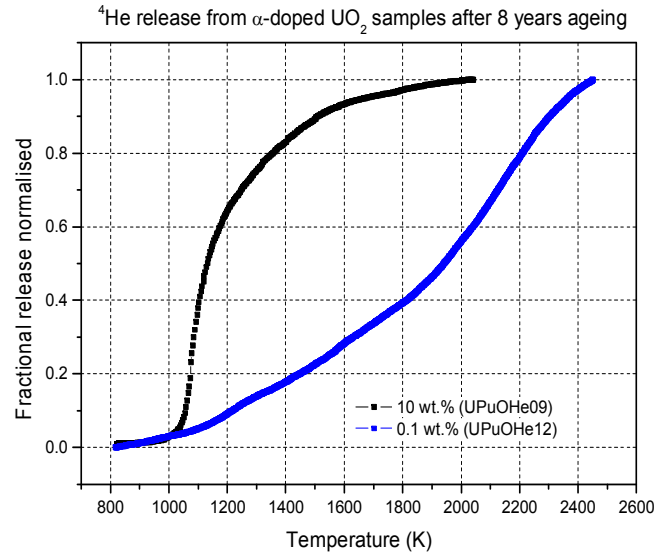
Sample



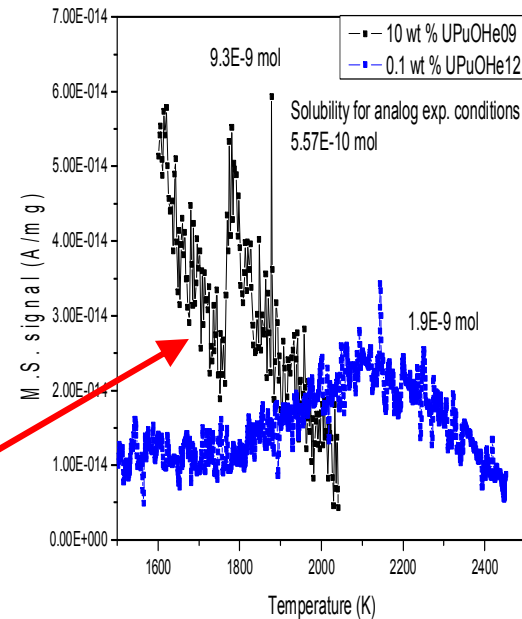
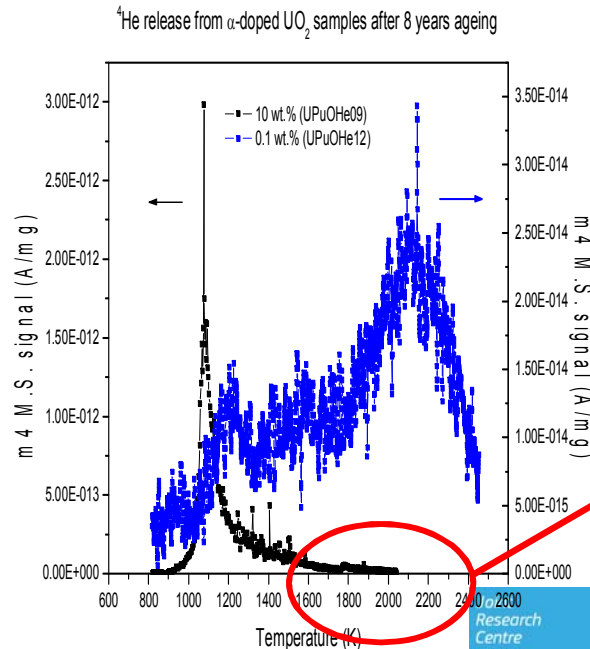
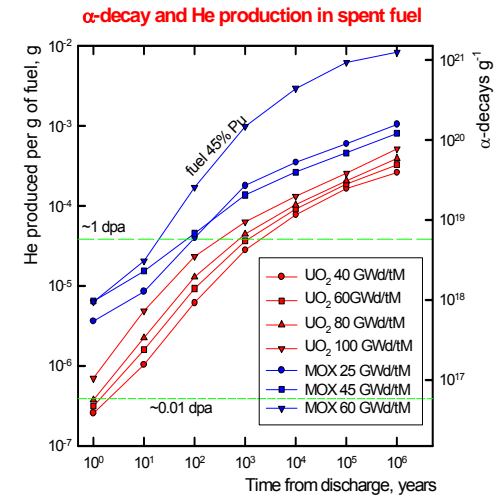
calibration



Helium release from 0.1 wt% ^{238}Pu -doped UO_2



The helium quantity released at higher temperature is close to the expected solubility.



He solubility in UO_2



Commission
européenne
Helium build up

